# Chemically Speciated Air Pollutant Emissions from Open Burning of Household Solid Waste from South Africa

Xiaoliang Wang[1], Hatef Firouzkouhi[1], Judith C. Chow[1], John G. Watson[1], Steven Sai Hang Ho[1], Warren Carter[2], Alexandra S.M. De Vos[2]

[1] Division of Atmospheric Sciences, Desert Research Institute, Reno, NV 89512, U.S.A.
[2] SASOL Research and Technology, Sasolburg, South Africa

*Correspondence to*: Xiaoliang Wang (xiaoliang.wang@dri.edu)

**Abstract**

Open burning of household solid waste is a large source of air pollutants worldwide, especially in the Global South~~developing countries~~. However, waste burning emissions are either missing or have large uncertainties in local, regional, or global emission inventories due to limited emission factor (EF) and activity data. Detailed particulate matter (PM) chemical speciation data is even ~~scarcer~~less available. This paper reports source profiles and EFs for $PM_{2.5}$ species as well as acidic and alkali gases measured from laboratory combustion of ten waste categories that represent open burning in South Africa. Carbonaceous materials contributed more than 70% of $PM_{2.5}$ mass. Elemental carbon (EC) was most abundant from flaming materials (e.g., plastic bags, textile, and combined materials) and its climate forcing exceeded the corresponding $CO_2$ emissions by a factor of 2–5. Chlorine had the highest EFs among elements measured by X-ray fluorescence (XRF) for all materials; vegetation emissions showed high abundances of potassium, consistent with its use as a marker for biomass burning. Fresh $PM_{2.5}$ emitted from waste burning appeared to be acidic. Moist vegetation and food discards had the highest hydrogen fluoride (HF) and PM fluoride EFs due to fluorine accumulation in plants, while burning rubber had the highest hydrogen chloride (HCl) and PM chloride EFs due to high chlorine content in the rubber. Plastic bottles, plastic~~and~~ bags, rubber, and food discards had the highest EFs for polycyclic aromatic hydrocarbons (PAHs) and nitro-PAHs as well as their associated toxicities. Distinct differences between odd and even carbon preferences were found for alkanes from biological and petroleum-based materials: dry vegetation, paper, textile, and food discards show preference for the odd-numbered alkanes, while the opposite is true for plastic bottles, plastic bags, and rubber. As phthalates are used as plasticizers, their highest EFs were found for plastic bottles and bags, rubber, and combined materials. Data from this study will be useful for health and climate impact assessments, speciated emission inventories, source-oriented dispersion models, and receptor-based source apportionment.

**1 Introduction**

30       Uncontrolled open burning is a common practice to dispose of household or municipal solid waste (MSW) in many rural communities, especially in ~~developing countries~~the Global South (Cook and Velis, 2021; Sharma et al., 2022; Okedere et al., 2019; Das et al., 2018; Bulto, 2020; Reyna-Bensusan et al., 2018; Cheng et al., 2020). While MSW incineration oxidizes nearly all fuel carbon to carbon dioxide ($CO_2$), open burning only fully oxidizes about 58% of the materials (IPCC, 2006). Open burning has lower combustion efficiencies due to inefficient mixing of fuels and oxygen and low burning temperatures,

35  resulting in emissions of a wide range of air pollutants (Velis and Cook, 2021). MSW is often burned close to community residences. The limited dispersion and dilution increase direct inhalation exposures and exacerbate adverse health effects (Wiedinmyer et al., 2014; Lemieux et al., 2004; Krecl et al., 2021). MSW open burning emissions deteriorate air quality in neighborhood-, urban-, and regional-scales (Oleniacz et al., 2023). Low-income Communities ~~with lower socioeconomic status~~ are often more impacted by MSW burning emissions, leading to environmental justice concerns (Nagpure et al., 2015;

40  Martuzzi et al., 2010). It is estimated that exposure to $PM_{2.5}$ from open burning of solid waste causes at least 270,000 premature deaths ~~per year~~ globally (Williams et al., 2019) and 10,000–20,000 premature deaths in Africa (Gordon et al., 2023; Kodros et al., 2016) each year. Open burning also contributes to climate change as a result of large carbon dioxide ($CO_2$) and light absorbing carbon (including black carbon [BC]) emissions, two of the largest climate forcers (IPCC, 2013; Reyna-Bensusan et al., 2018; Bond et al., 2013).

45      Despite the large environmental impacts of uncontrolled MSW open burning, its emissions are not included or are poorly represented in local, regional, and global emission inventories due to lack of emission factor (EF) and amount of MSW burned (activity) data (Cook and Velis, 2021; Ramadan et al., 2022). Most existing inventories only include criteria pollutants (U.S. EPA, 2023) or greenhouse gases (IPCC, 2006) with limited chemical speciation. In addition to criteria pollutants, solid waste burning emits other toxic compounds. Construction timber combustion releases high concentrations of arsenic (As), chromium

50  (Cr), and copper (Cu), while plastic burning releases phthalates, polycyclic aromatic hydrocarbons (PAHs), and dioxins (Velis and Cook, 2021; Wasson et al., 2005). Lemieux (1997, 1998) reported gas and speciated particle emissions from simulated open burning of household waste in barrels. However, the study was limited to testing U.S. households with and without recycling practices. Barrel burning may not represent open pile burning due to different fuel-air interactions. Lemieux et al. (2004) further summarized organic air toxics from open burning of many materials, including MSW, and these data are used

55  in the US Environmental Protection Agency (US EPA) AP-42 Compilation of Air Emissions Factors (U.S. EPA, 1992). Stockwell (2016) measured emissions from laboratory burning of shredded tires, plastic bags, mixed waste, and a variety of biomass species. Gaseous chemical EFs were presented, but PM chemistry was not reported. Jayarathne et al. (2018) reported EFs for $PM_{2.5}$ (particles with aerodynamic diameter ≤2.5 μm) and several components (carbon, ions, metals, and organics) for combustion sources in Nepal, including mixed waste under dry and damp conditions, two types of plastic mixtures, and crop

60  residues. Emissions of criterial pollutants and $PM_{2.5}$ compositions (carbon, ions, and metals) were reported for several types of MSW in China (Cheng et al., 2020). Several studies characterized PM mass and chemistry for plastics burning (Hoffer et

al., 2020; Wu et al., 2021). These studies highlighted ~~the~~a large variation of EFs due to the heterogeneities in waste compositions and burning conditions.

Detailed PM chemical composition~~s~~ data are important for many applications. The association between PM mass exposure and mortality is well established and exposure to $PM_{2.5}$ is one of the most important risk factors for premature death in the global burden of disease (Murray et al., 2020). However, as PM is a complex mixture, the toxicity and carcinogenicity of different chemical species are still uncertain (Lighty et al., 2000; Kelly and Fussell, 2012). Epidemiology and toxicology studies of PM chemicals are needed to develop a mechanistic understanding of their health effects. PM compositions are also used to evaluate visibility and climate effects. PM light scattering and absorption properties depend on the hygroscopicity and optical properties of its chemical components ~~composition and associated hygroscopicity and optical properties~~ (Watson, 2002). BC, or elemental carbon (EC), is the major light absorbing component of PM and may have a global warming potential 900 times that of $CO_2$ (Bond et al., 2013). Speciated emission inventories have been applied in source-oriented dispersion models to estimate ambient concentrations and deposition patterns and to target effective emission reduction strategies (Reff et al., 2009; Simon et al., 2010). Deposition from MSW burning emissions is a major cause of discoloring of the Taj Mahal in India (Lal et al., 2016). PM chemical composition is necessary for receptor-based source apportionment, which uses the chemical abundance patterns in source profiles to quantify contributions of different sources to ambient PM concentrations (Watson et al., 2016). The source profile collinearities caused by similarities is a major cause of source apportionment uncertainty. Extending chemical analyses beyond conventionally analyzed elements and ions to include particle-phase organics can potentially provide molecular markers to minimize collinearities.

This study used comprehensive laboratory combustion experiments to quantify emissions from ten types of MSW from South Africa. EFs for $CO_2$ and criteria air pollutants have been reported by Wang et al. (2023). This paper focuses on speciated source profiles and EFs for ~~including~~ elements, acidic and alkali gases and ions, PAHs, nitro-PAHs, n-alkanes, and phthalates.

## 2 Methodology

### 2.1 Waste Materials and Combustion Experiments

MSW materials were collected from typical household refuses by SASOL, a petrochemical and energy company, in the Zamdela community in South Africa. This is part of SASOL's Waste Collection Interventions (WCI) program to assist local communities in MSW collection and disposal in landfills to reduce illegal open burning and improve air quality. The materials were sent to the Desert Research Institute (DRI) in Reno, Nevada, USA for emission testing. Due to customs restriction and potential deterioration during shipping, the compositions of food discards and vegetation collected by the WCI were characterized and similar mixtures were collected in Nevada for testing. Food discards included bread, potato and banana peels, lettuce, cucumbers, and tomatoes (Cronjé et al., 2018) and vegetation included basin wild rye, Sandberg bluegrass, crested wheat grass, red willows, and creeping wild rye, representing African bunch grasses, African sumac, and crab grass. ~~samples were collected in Nevada to avoid deterioration during shipping.~~ The ten types of waste categories tested include: 1)

paper; 2) leather/rubber; 3) textile; 4) hard plastic bottles and food containers; 5) soft plastic bags; 6) dry vegetation (0% moisture content); 7) natural vegetation (20% moisture content); 8) damp vegetation (50% moisture content); 9) food discards; and 10) combined materials. The combined materials were mixtures of all categories based on their mass fractions in MSW. Glass, metals, and ceramics were added to the combination to mimic their influences on burning emissions. Moisture contents were measured right after collection in the field. The moisture contents for paper, leather/rubber, textile, and plastics were determined by a laboratory in South Africa by measuring the mass loss gravimetrically after heating a small fraction of samples at 103 °C for 30 minutes. The moisture contents for food and vegetation were determined at DRI by baking the samples at 90 °C for 24 hours. Because material moisture content will likely change during transport and storage, to represent field conditions, Before testing, the waste materials (except food discards) were oven dried at 90 °C for 24 hours, rehydrated to their natural moisture levels with distilled deionized water (DDW), and re-equilibrated for at least 24 hours before testing.

The major elemental compositions (i.e., carbon [C], hydrogen [H], nitrogen [N], sulfur [S], and oxygen [O]) of the waste materials were measured by an elemental analyzer (Model Flash EA1112, Thermo Scientific). The carbon content was used for the fuel-based EF calculation. The same procedure was used to quantify the elemental compositions of ashes after combustion.
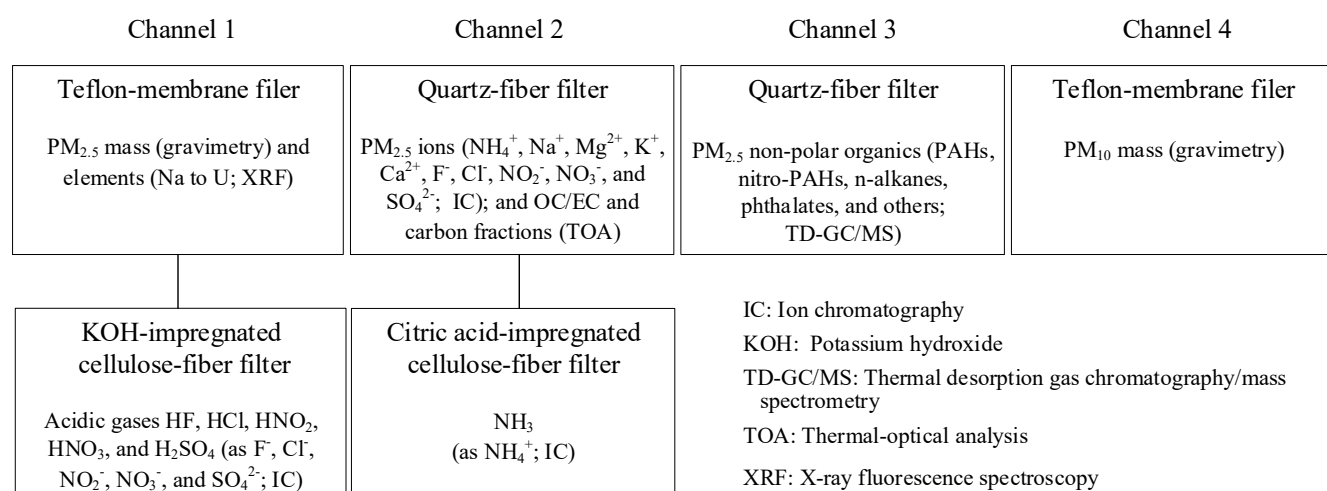
**Figure 1: Analyses for the three PM$_{2.5}$ and one PM$_{10}$ filter channels.**

The experimental method has been documented by Wang et al. (2023) and only a brief description is provided here. For each burn, 0.5 to 20 g of waste material was placed in a ceramic crucible and maintained at 450 °C to simulate open burning. Each burn typically took 30 min1800 s, varying from 161000 to 654000 smin. Paper, textile, soft plastic bags, vegetations (with dry and natural moisture contents), and combined waste had both flaming and smoldering phases, while leather/rubber, plastic bottles, damp vegetation, and food discards only smoldered. A suite of gas and particle analyzers monitored the concentrations in real time, including CO$_2$, carbon monoxide (CO), oxides of nitrogen (NO$_x$), sulfur dioxide (SO$_2$), PM$_{2.5}$, and

PM$_{10}$ (particles with aerodynamic diameter ≤10 μm). Integrated PM samples were collected simultaneously onto four parallel filters that accommodated different chemical analyses (Figure 1~~Figure 1~~). A total of 29 filter sets were collected, including three replicates for each of the eight fuels, two replicates for vegetations with 20% and 50% moisture content, and one field blank.

**2.2 Chemical Analysis**

As shown in Figure 1~~Figure 1~~, the PM$_{10}$ filters (Channel 4) were weighed for gravimetric mass concentrations, while the three PM$_{2.5}$ filters (Channels 1–3) were analyzed for elements, ions, carbon fractions, and organic compounds (Chow and Watson, 2013). Back-up filters impregnated with gas-absorbing solutions were analyzed for acidic and alkali gases.

Channel 1 is a Teflon-membrane filter backed by a potassium hydroxide (KOH)-impregnated cellelose-fiber filter. The Teflon-membrane filters were analyzed for PM$_{2.5}$ mass by gravimetry using microbalances (Model XP-6, Mettler Toledo, Hightstown, NJ) with 1 μg sensitivity (Watson et al., 2017). In addition, 51 elements (from Na to U) were measured using a PANalytical X-ray fluorescence (XRF) analyzer (Model Epsilon 5, Almelo, The Netherlands) (Watson et al., 1999). The backup KOH-impregnated cellelose-fiber filters behind the Teflon-membrane front filter were analyzed for acidic gases, including hydrogen fluoride (HF), hydrochloric acid (HCl), nitrous acid (HNO$_2$), nitric acid (HNO$_3$), and sufuric acid (H$_2$SO$_4$) as their corresponding ions (i.e., F$^-$, Cl$^-$, NO$_2^-$, NO$_3^-$, and SO$_4^{2-}$) by ion chromatography (IC) (Sturges and Harrison, 1989; Eldering et al., 1991), which are known to emit from waste burning (Christian et al., 2010).

Channel 2 contains a quartz-fiber filter backed by a citric acid-impregnated cellelose-fiber filter. Half of the quartz-fiber filter was extracted in DDW and analyzed for ten water-soluble ions, including: ammonium (NH$_4^+$), sodium (Na$^+$), magnesium (Mg$^{2+}$), potassium (K$^+$), calcium (Ca$^{2+}$), fluoride (F$^-$), chloride (Cl$^-$), nitrite (NO$_2^-$), nitrate (NO$_3^-$), and sulfate (SO$_4^{2-}$) by using Dionex ICS 6000 IC systems (Thermo Scientific, Sunnyvale, CA) (Chow and Watson, 2017). The backup citric acid-impregnated cellelose-fiber filter behind the quartz-fiber front filter was anlayzed for ammonia (NH$_3$) as NH$_4^+$ by IC.

Organic and elemental carbon (OC and EC), and eight thermal fractions (i.e., OC1–OC4, pyrolyzed carbon [OP], EC1–EC3) were quantified following the IMPROVE_A thermal/optical protocol using the DRI Model 2015 Multiwavelength Carbon Analyzer (Magee Scientific, Berkeley, CA) (Chow et al., 2007; 2015b; Chen et al., 2015). A 0.5 cm$^2$ punch was taken from the Channel 2 quartz-fiber filter and heated in a pure helium (He) carrier gas at 140 ℃ (OC1), 280 ℃ (OC2), 480 ℃ (OC3), and 580 ℃ (OC4) temperature steps. Next, the carrier gas composition was changed to 98% He/2% O$_2$, and the filter continued to be heated at 580 ℃ (EC1), 740 ℃ (EC2), and 840 ℃ (EC3). Seven lasers with wavelengths ranging from 405 nm to 980 nm were used to monitor light reflectance (R) and transmittance (T), which were used to calculate wavelength dependent light absorption. OC and EC were determined at the 635 nm wavelength after R returned to its initial value to correct for OC pyrolysis. The multiwavelength measurement allowed separation of light absorption by black carbon (BC) from brown carbon (BrC), which has unique wavelength dependence based on fuel and combustion conditions (Chow et al., 2015b; 2018; 2021).

A parallel quartz-fiber filter in Channel 3 was analyzed for non-polar organic compounds, including PAHs, nitro-PAHs, alkanes, cycloalkanes, hopanes, steranes, phthalates, and other organics using in-injection port-thermal desorption-gas chromatography mass spectrometry (TD-GC/MS) (Ho et al., 2008; Ho and Yu, 2004; Ho et al., 2011). Aliquots (1.0–1.5 cm$^2$) of the quartz-fiber filters were cut into small pieces, spiked with internal standards, and inserted into TD tubes for analyses.

Chemical data were quality checked as part of quality assurance (QA) to ensure internal consistency and to achieve mass closure. As shown in Supplemental Figure S1, the sum of measured chemical species and reconstructed mass accounted for 73% and 99% of gravimetric mass on average, respectively. High coefficients of determination ($R^2$) of 0.98 assure that major PM$_{2.5}$ constituents (i.e., gravimetric mass, carbon, ions, and elements) are quantified with high quality (Chow et al., 2015a). To obtain chemical source profiles, the chemical concentrations were normalized to PM$_{2.5}$ mass concentrations. Potential markers and hazardous air pollutants emissions from each waste category were assessed. Fuel-based EFs were calculated based on carbon mass balance techniques (Wang et al., 2023).

## 3 Results and Discussion

### 3.1 Major PM$_{2.5}$ Compositions

Figure 2~~Figure 2~~ compares average PM$_{2.5}$ mass fractions for the five major composition categories (i.e., organic matter OM, EC, ions, mineral, and others). Carbonaceous aerosol (OM and EC) contributed more than 70% of PM$_{2.5}$ mass with minor contributions from ions. OM was the most abundant component, accounting for >50% of PM$_{2.5}$ mass. EC had the highest abundances in the flaming materials, including plastic bags (49.4±29.2%), combined fuels (47.9±13.2%), textile (12.8±4.3%), and dry vegetations (9.1±2.2%). Detailed mass fractions for each material are shown in Figure S2. High OC and EC abundances were also found for PM$_{2.5}$ from waste burning in other studies. ~~of mixed waste and plastics in Nepal (Jayarathne et al., 2018) and China (Wu et al., 2021; Cheng et al., 2020).~~ For example, Jayarathne et al. (2018) found average OC and EC abundances of 77% (ranging 59–114%) and 2.6% (ranging 0–12%), respectively, for mixed waste in Nepal. Wu et al. (2021) found carbonaceous components were 80.5–91.4% of PM$_{2.5}$ for flaming burning of various plastics in China, with OC and EC ranging 45–63% and 7–53%, respectively, which are similar to the flaming emissions in this study.

The abundances of the seven carbon fractions (i.e., OC1–OC4 and EC1–EC3) by source type are shown in Figure S3. The sum of lower temperature OC1 and OC2 fractions exceeded 20% for most fuels, except for plastic bags and combined materials that had intense flaming combustion. Paper and vegetation had higher OC3+OC4 fractions (15–30%), consistent with their higher charring fractions (pyrolysis of OC to EC during oxygen-free heating). Plastic bags and combined materials had the highest sums of EC1 and EC2 (53–70%), with plastic bags having much higher EC2 (63%) than EC1 (8%), indicating higher combustion temperatures. High temperature EC3 (840ºC) were not detected. Carbon fractions varied by moisture content in vegetation samples with the highest OC3, OC4, and EC1 in dry vegetation due to dominant flaming combustion. As moisture content increased to 50%, the abundances of OC1 increased, OC2 remained approximately the same, while OC3, OC4, and

EC1 abundances decreased. Similar carbon fraction distributions were found for barrel and pile burning of MSW by Cheng et
180  al. (2020).
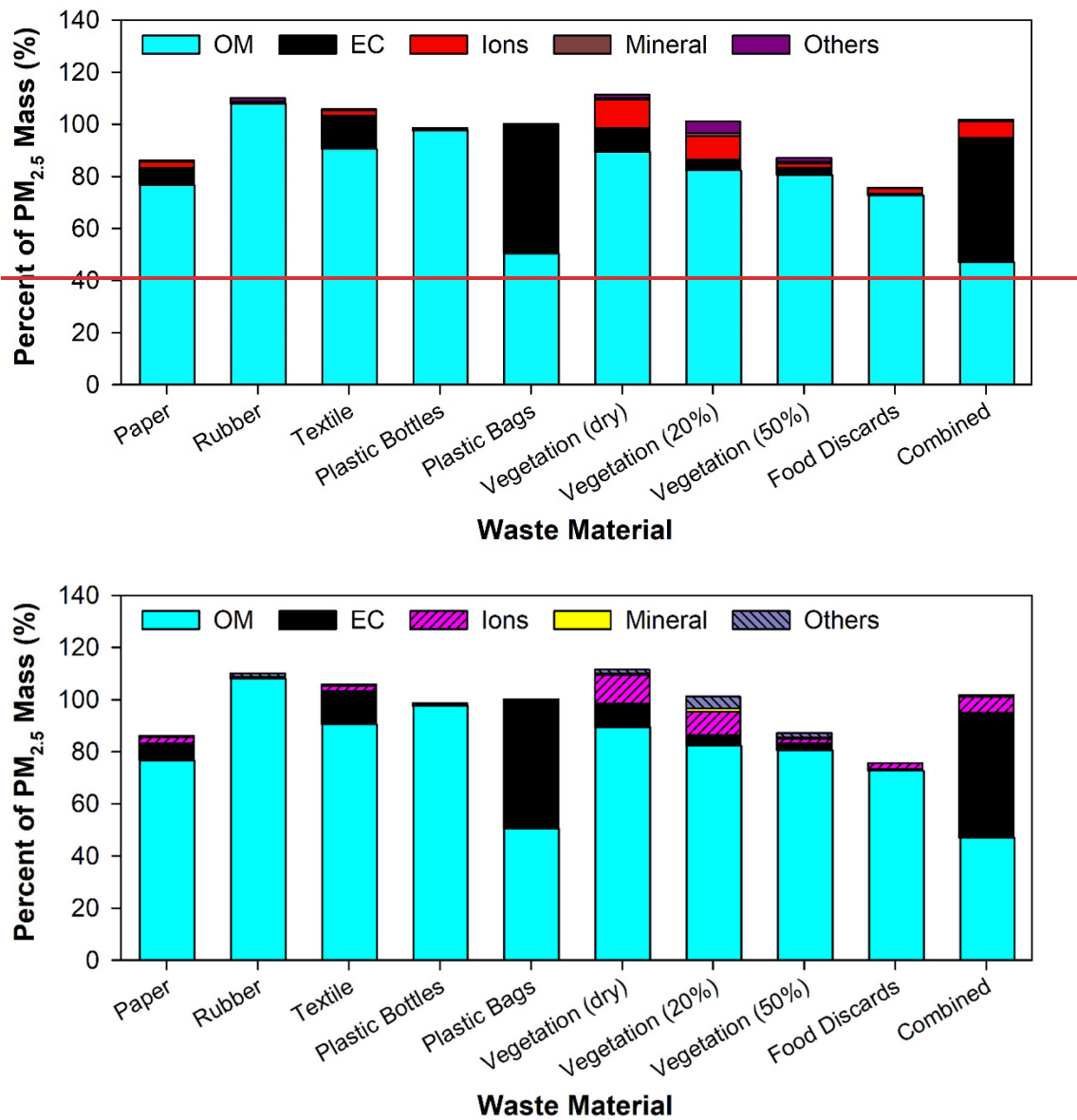
**Figure 2: Abundances of major PM$_{2.5}$ compositions (percent of PM$_{2.5}$ mass) from burning of different waste materials. (oOrganic matter OM = OC × 1.4; ions is the sum of ammonium (NH$_4^+$), sodium (Na$^+$), magnesium (Mg$^{2+}$), potassium (K$^+$), calcium (Ca$^{2+}$),**
185  **fluoride (F$^-$), chloride (Cl$^-$), nitrite (NO$_2^-$), nitrate (NO$_3^-$), and sulfate (SO$_4^{2-}$) by IC; minerals = 2.2×Al + 2.49×Si + 1.63×Ca + 2.42×Fe + 1.94×Ti. See detailed description of the major composition categories in Supplemental Materials S1.**

Figure 3Figure 3 shows EFs for PM$_{2.5}$ and its major components OM and EC. Rubber, plastic bottles, 50% moisture

vegetation, and food discards generated higher EFs for PM$_{2.5}$ and OM among 10 source types, consistent with their dominant

smoldering combustion. Combustion of plastic bottles produced the highest EFs for $PM_{2.5}$ (651 ± 38 g $kg^{-1}$) and OM (635 ±
49 g $kg^{-1}$). As shown in Figure S2d, over 97% of the plastic bottle $PM_{2.5}$ is OM. Rubber had the second highest EFs for $PM_{2.5}$
(141 ± 23 g $kg^{-1}$) with 98% $PM_{2.5}$ mass being OM (Figure S2b). Plastic bags had the highest EFs for EC (17.1 ± 1.9 g $kg^{-1}$),
followed by textile (5.52 ± 0.24 g $kg^{-1}$) and combined waste materials (3.44 ± 1.98 g $kg^{-1}$). Assuming a 100-year global
warming potential (GWP) of 900 for EC (Bond et al., 2013), the climate forcing of EC from these materials is a factor of 2–5
higher than that of $CO_2$ (Wang et al., 2023).

As 50% moisture vegetation only smoldered, the $PM_{2.5}$ EF (88 ± 7 g $kg^{-1}$) was over an order of magnitude higher than
those of dry (3.2 ± 1.3 g $kg^{-1}$) and 20% moisture (4.8 ± 2.0 g $kg^{-1}$) samples. Even though the dry vegetation had a higher EC
abundance than the 50% moisture vegetation (8.2% vs. 2.6% of $PM_{2.5}$), the 50% moisture vegetation still had a higher EF for
EC due to the much higher EF for $PM_{2.5}$ (Figure 3). Pokhrel et al. (2021) reported PM (≤720 nm) EFs for seven types of
African woody biomasses, averaging 19.2 (ranging 13.2–25.1) g $kg^{-1}$ for burns with MCE <0.85, which is lower than that for
the 50% moisture sample in this study; on the other hand, PM EFs were 5.0 (ranging 0.82–22.2) g $kg^{-1}$ for burns with
MCE≥0.85, which are similar to those for the dry and 20% moisture samples.
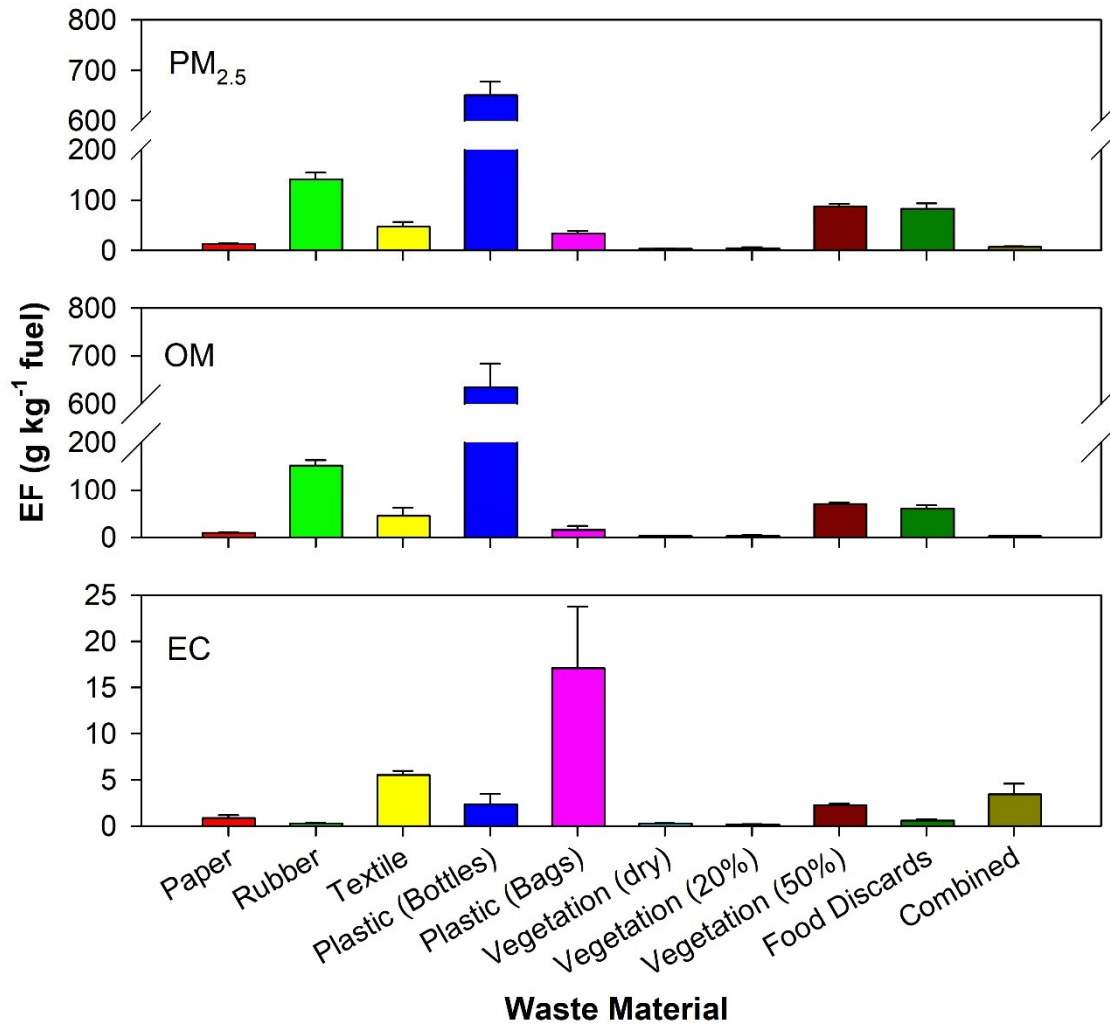
**Figure 3: Emission factors for PM2.5, organic matter (OM= OC × 1.4), and elemental carbon (EC). The error bars represent the larger of the propagated analytical uncertainty or the standard error of multiple runs.**

As thermal EC and optical BC are often used interchangeably (Pöschl, 2003), Table 1 compares EC from this study with EC or BC reported in the literature. The EC EF for paper ($0.86 \pm 0.57$ g kg$^{-1}$) is in the same range as those ($0.5$–$0.76$ g kg$^{-1}$) reported by Cheng et al. (2020) and Wu et al. (2021), while the EF for textile is about 4 times those reported by Cheng et al. (2020). A wide range of EFs are reported for plastic bottles and bags. The plastic bag EF ($17.1 \pm 11.6$ g kg$^{-1}$) is in good agreement with plastic foam ($18.7 \pm 3.9$ g kg$^{-1}$) by Wu et al. (2021) and close to a plastic mixture ($10.3 \pm 1.0$ g kg$^{-1}$) burned by Jayarathne et al. (2018). Different vegetation types, moisture contents, and burning conditions resulted in variable EFs. However, EFs for this study fall in the range reported by Akagi et al. (2011) except for 50% moisture vegetation that is 75% higher than the maximum value by Akagi et al. (2011). Andreae (2019) summarized emissions from biomass burning for Savanna/grassland, tropical/temperate/boreal forest, and agricultural residue fuels and reported average BC EFs of 0.42–0.55.

The EF for mixed materials (3.44± 1.98 g kg$^{-1}$) is similar to those reported for damp mixed garbage (3.30 ± 3.88 g kg$^{-1}$) in Nepal (Jayarathne et al., 2018; Stockwell et al., 2016) but is five times the suggested value (0.65 ± 0.27 g kg$^{-1}$)  for global emission inventory (Akagi et al., 2011; Wiedinmyer et al., 2014). The high variability of the BC EFs (1.4± 5.1 g kg$^{-1}$) for mixed waste burning is also shown  by Andreae (2019), due to different materials, burning conditions, and limited number of studies.

Table 1: Comparison of EC or BC and PAH emission factors measured in this study with those from the literature.

| Ref. | Region | Fuel | Method | EC or BC (g kg$^{-1}$ fuel) | PAHs (g kg$^{-1}$ fuel) |
|---|---|---|---|---|---|
| **Paper** | | | | | |
| **This study** | **South Africa** | **Paper** | **Lab burning** | **0.86 ± 0.57** | **0.051 ± 0.001** |
| (Park et al., 2013) | South Korea | Paper | Lab incinerator | | 0.002 |
| (Hoffer et al., 2020) | Hungary | Advertising flyer and newspaper | Lab stove | | 0.0012 ± 0.0008 |
| (Cheng et al., 2020) | China | Paper | Lab barrel | 0.76 ±0.01 | |
| (Cheng et al., 2020) | China | Paper | Lab pile | 0.50 ±0.02 | |
| (Wu et al., 2021) | China | Paper packaging | Field | 0.50 ± 0.11 | 0.031 ± 0.018 |
| **Leather/Rubber** | | | | | |
| **This study** | **South Africa** | **Synthetic car floor mat** | **Lab burning** | **0.29 ± 0.08** | **1.41 ± 0.06** |
| (Hoffer et al., 2020) | Hungary | Tire | Lab stove | | 0.025 ± 0.009 |
| **Textile** | | | | | |
| **This study** | **South Africa** | **Cloth** | **Lab burning** | **5.52 ± 0.24** | **0.015 ± 0.005** |
| (Hoffer et al., 2020) | Hungary | Cloth | Lab stove | | 0.021 ± 0.019 |
| (Cheng et al., 2020) | China | Textile | Lab barrel | 1.47 ± 0.13 | |
| (Cheng et al., 2020) | China | Textile | Lab pile | 1.30 ±0.09 | |
| **Plastics** | | | | | |
| **This study** | **South Africa** | **Plastic bottles** | **Lab burning** | **2.37 ± 1.89** | **8.55 ± 2.02** |
| **This study** | **South Africa** | **Plastic bags** | **Lab burning** | **17.1 ± 11.6** | **0.24 ± 0.04** |
| (Park et al., 2013) | South Korea | Plastics | Lab incinerator | | 0.007 |
| (Jayarathne et al., 2018) | Nepal | Chip bags (damp) | Field | 5.71 ± 0.58 | 0.076 |

| Ref. | Region | Fuel | Method | EC or BC (g kg$^{-1}$ fuel) | PAHs (g kg$^{-1}$ fuel) |
|---|---|---|---|---|---|
| (Jayarathne et al., 2018) | Nepal | Plastics (mostly heavy clear plastic, some plastic cups, and food bags) | Field | 10.31 ± 1.04 | 0.152 |
| (Hoffer et al., 2020) | Hungary | Different types of plastics | Lab stove | | 0.03–0.26 |
| (Wu et al., 2021) | China | Plastic packaging | Field | 0.22–0.70 | 0.017–0.03 |
| (Wu et al., 2021) | China | Plastic foam | Field | 18.7 ± 3.9 | 0.256 ± 0.093 |
| **Vegetation** | | | | | |
| **This study** | **South Africa** | **Vegetation (0% H$_2$O)** | **Lab burning** | **0.27 ± 0.03** | **0.010 ± 0.004** |
| **This study** | **South Africa** | **Vegetation (20% H$_2$O)** | **Lab burning** | **0.19 ± 0.04** | **0.001±0.001** |
| **This study** | **South Africa** | **Vegetation (50% H$_2$O)** | **Lab burning** | **2.28 ± 0.21** | **0.046 ± 0.003** |
| **This study** | **South Africa** | **Food discards** | **Lab burning** | **0.60 ± 0.25** | **0.173 ± 0.069** |
| (Christian et al., 2010) | Mexico | Cooking biofuels | Field/Lab | 0.205–0.674 | |
| (Akagi et al., 2011) | Worldwide | Biomass | Data Synthesis | 0.2–1.3 | |
| (Park et al., 2013) | South Korea | Wood | Lab incinerator | | 0.001 |
| (Jayarathne et al., 2018) | Nepal | Crop residue (Rice, wheat, mustard, lentil, & weed grass) | Field | 0.98 ± 0.12 | 0.011 |
| (Andreae, 2019) | Worldwide | Savanna/grassland, tropical/temperate/boreal forest, agricultural residues | Data Synthesis | 0.42–0.55 | 0.012–0.72 |
| (Wu et al., 2021) | China | Organic waste | Field | 0.54 ± 0.39 | 0.032 ± 0.014 |
| **Mixed household waste** | | | | | |
| **This study** | **South Africa** | **Mixed garbage** | **Lab burning** | **3.44 ± 1.98** | **0.024 ± 0.010** |
| (Lemieux, 1997) | U.S. | Recycler waste | Lab barrel | | 0.0235–0.0244 |
| (Lemieux, 1997) | U.S. | Non-recycler waste | Lab barrel | | 0.0497–0.0824 |
| (Christian et al., 2010) | Mexico | Landfill MSW | Field | 0.381–0.924 | |
| (Akagi et al., 2011; Wiedinmyer et al., 2014) | U.S. and Mexico | Mixed waste | Data Synthesis | 0.65 ± 0.27 | |
| (Park et al., 2013) | South Korea | Domestic municipal solid waste | Lab incinerator | | 0.0015 |
| (Stockwell et al., 2016) | Nepal | Mixed waste | Field | 3.30 ± 3.88 | |
| (Jayarathne et al., 2018) | Nepal | Dry mixed garbage | Field | <0.04 | 0.015 |
| (Jayarathne et al., 2018) | Nepal | Damp mixed garbage | Field | 1.56–3.41 | 0.097–0.149 |

| Ref. | Region | Fuel | Method | EC or BC (g kg$^{-1}$ fuel) | PAHs (g kg$^{-1}$ fuel) |
|---|---|---|---|---|---|
| (Andreae, 2019) | Worldwide | Mixed garbage | Data Synthesis | 1.4 ± 5.1 | 0.011–0.045 |
| (Cheng et al., 2020) | China | Mixed waste | Lab barrel | 1.26 ± 0.16 | |
| (Cheng et al., 2020) | China | Mixed waste | Lab pile | 1.03 ±0.13 | |

### 3.2 Elements

Figure 4Figure 4 shows EFs for elements measured by XRF with EF values larger than uncertainties for at least three of the ten waste materials or those in the Hazardous Air Pollutants (HAPs) list of the U.S. Environmental Protection Agency

225    (U.S. EPA, 2020). Chlorine (Cl) had the highest EFs for all waste materials. Rubber had the highest EFs for Cl and sulfur (S) as well as HAP elements cadmium (Cd), antimony (Sb), and lead (Pb), while the 50% moist vegetation had the highest EFs for chromium (Cr), cobalt (Co), nickel (Ni), and selenium (Se). Table S2 compares these heavy metal EFs with those reported in the literature. The EFs by Park et al. (2013) are lower than those by other studies for most elements, except for higher zinc (Zn) EFs. For paper burning, both this study and Cheng et al. (2020) found similar EFs for copper (Cu) and Pb. The plastic

230    bottles had much higher EFs for Cr and Pb than plastic bags and other studies; high Cu EFs for plastics are also found from this study and Cheng et al. (2020). The high Cu emissions from paper and plastics likely originate from the Cu compounds used for cyan, green and reddish blue printing pigment (Zięba-Palus and Trzcińska, 2011). The EFs for Cr, Zn, and Pb from dry and 20% moisture vegetations are similar to those by Cheng et al. (2020), while the Cu EFs for 50% moisture vegetation is similar to that by Cheng et al. (2020). For the combined materials, Cr and Ni are below detection limits in this study, but

235    the EFs for other elements are in the same range as those reported in the literature, with large variations (Lemieux, 1997; Christian et al., 2010; Jayarathne et al., 2018; Cheng et al., 2020).

The elemental abundances are shown in Figure S4. Cl abundance ranged from 0.04±0.04% of PM$_{2.5}$ mass for plastic bags to 5.1±4.3% for dry vegetation. The low Cl abundance in the tested plastics was probably due to their lack of polyvinyl chloride (PVC) components. Vegetation samples had higher potassium (K) abundances, consistent with the fact that K is often used as

240    a biomass burning marker. Plastic bottles and bags had lower abundances of most elements than other materials, similar to the findings by Valavanidis et al. (2008). Sb has been reported as a potential marker for solid waste burning because of its use in textile (flame retardant), batteries, and polyethylene terephthalate (PET) projection (Jayarathne et al., 2018; Christian et al., 2010). Figure S4 shows that Sb had higher abundances in rubber, vegetation, and mixed materials, but with lower abundances in paper, plastics, and food discards, indicating that caution should be taken when using Sb as a waste burning marker due to

245    its high dependence on waste compositions. The Sb abundance in the combined materials (0.035±0.021%) is similar to the value of 0.025±0.033% reported by Jayarathne et al. (2018). The combined materials had higher abundances of Pb (0.075±0.062%) than other waste categories, probably related to the metals and glass added to the mix; this value is similar to 0.057±0.077% reported by Jayarathne et al. (2018).
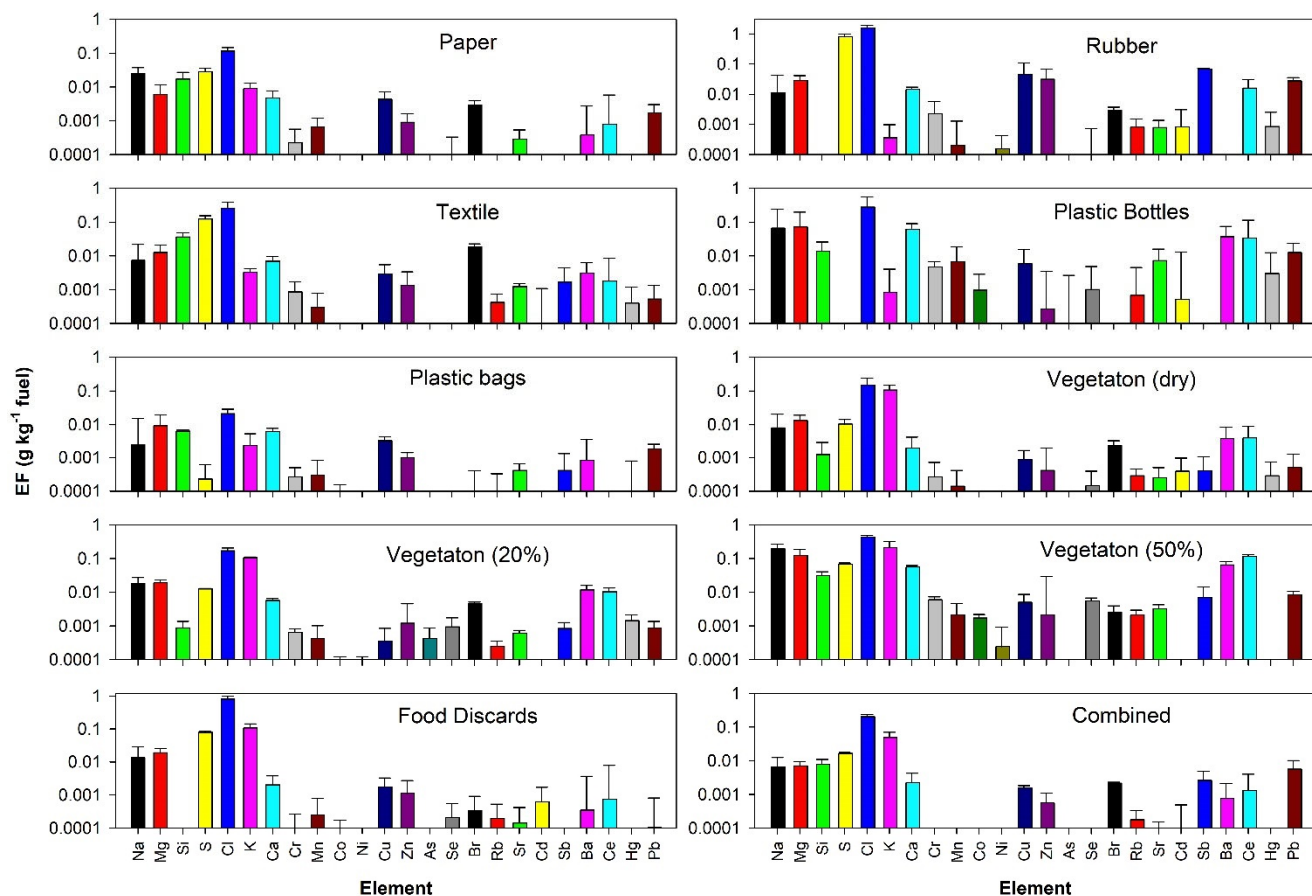
**Figure 4: Emission factors for key elements.**

### 3.3 Acidic and Alkali Gases and Ions

Acidic and alkali ionic species are present in both gas and particle phases and their partition depends on temperature and reactions. Acidic and alkali gases are toxic and corrosive; they can cause adverse effects on human health, materials, and ecosystems if not neutralized soon after emission. Figure S5 shows elevated ionic concentrations for $NO_3^-$ and $NH_4^+$ on backup filters (i.e., in the form of $HNO_3$ and $NH_3$, respectively). The sum of gaseous ion abundances ranged from 0.6% (plastic bottles) to 73% (dry vegetation) of $PM_{2.5}$, higher than the particulate ions abundances (less than 10% of $PM_{2.5}$). Figure S6 shows abundant $Cl^-$ and $SO_4^{2-}$ for dry and 20% vegetation. Consistent with high abundances of elemental K, dry and 20% moisture vegetation show high $K^+$ abundances. Vegetation with 50% moisture content had low $K^+$ abundances, probably because the dominant smoldering phase left most K in the ash. The sums of anion equivalents were higher than those for cations for most materials, likely because hydrogen ion ($H^+$) was not measured; it might be associated with hydrochloric, sulfuric, or nitric acids. Therefore, directly emitted particles appear to be acidic, although these would probably be neutralized by available $NH_3$

soon after emission. The deposition of the acidic waste burning particles probably contributed to discoloring of the Taj Mahal in India (Lal et al., 2016).

Figures 5 and 6 show that EFs for HCl from rubber; $HNO_3$ from rubber, textile, vegetation, and food discards; and $NH_3$ from food discards were one to two orders of magnitude higher than the corresponding particulate ions. Food discards and 50% moisture vegetation had the highest EFs for HF and particulate $F^-$, consistent with fluorine accumulation in plants (Jayarathne et al., 2014). The modified combustion efficiencies (MCEs) for the dry (MCE = 0.88) and 20% moisture (MCE = 0.91) vegetation samples were higher than the 50% moisture vegetation sample (MCE = 0.79) (Wang et al., 2023). One would expect that the dry and 20% moisture vegetation samples would cause higher EFs for HF than particulate $F^-$ due to preferred partition in the gas phase at higher combustion temperatures and MCEs. However, low HF and $F^-$ EFs were observed in these cases. Future study should investigate the partitioning of fluorine among gases, particles, and ashes during biomass burning. Jayarathne et al. (2014) reported $F^-$ EFs in the range of 0.7–136 mg kg$^{-1}$ for several types of biomass burning with an overall average of $32 \pm 7$ mg kg$^{-1}$. These values are in the range of dry ($7.6 \pm 0.6$ mg kg$^{-1}$) and 25% moisture vegetations ($17.8 \pm 8.3$ mg kg$^{-1}$), but lower than the 50% moisture vegetation ($744 \pm 61$ mg kg$^{-1}$) and food discards ($291 \pm 88$ mg kg$^{-1}$).

The rubber sample had the highest EF for HCl ($9.6 \pm 1.5$ g kg$^{-1}$) with an order of magnitude lower EF for PM $Cl^-$ ($0.8 \pm 0.2$ g kg$^{-1}$). Consistent with low elemental Cl emission, the plastic bottles or bags did not have high HCl or $Cl^-$ emissions. Lemieux (1997) reported HCl EFs of 1.51–3.28 and 0.086–0.481 g kg$^{-1}$ for combined waste materials with higher and lower PVC mass fractions, respectively. The EF for lower PVC waste is similar to the values for combined materials ($0.47 \pm 0.22$ g kg$^{-1}$) measured in this study. These values are lower than the 1.7–9.8 g kg$^{-1}$ EFs reported by Christian et al. (2010) for landfill MSW burning in Mexico. Stockwell et al. (2016) measured HCl from six mixed garbage samples and found EFs ranging from non-detectable to 3.03 g kg$^{-1}$. They also found that one sample containing mostly plastic bags did not have detectable HCl but another sample dominated by hard plastics had a high HCl EF of 77.9 g kg$^{-1}$, indicating the high sensitivity of HCl EFs to fuel compositions.

Due to high volatilities, $NO_2^-$ and $NO_3^-$ were in the gas phase (Figure S5). The waste materials had low sulfur contents (Wang et al., 2023); therefore, EFs for both $H_2SO_4$ and $SO_4^{2-}$ were low. $NH_3$ was in gas phase because the fresh emissions had not reacted with acidic gases to create PM ammonium. Similar to HF emissions, 50% moisture vegetation ($2.86 \pm 0.16$ g kg$^{-1}$) and food discards ($6.98 \pm 1.05$ g kg$^{-1}$) had the highest $NH_3$ EFs. The $NH_3$ EFs for the combined materials was $0.23 \pm 0.08$ g kg$^{-1}$, within the large variations of $0.94 \pm 1.02$ g kg$^{-1}$ reported by Akagi et al. (2011). The $NH_3$ EFs for the vegetations (0.29–2.86 g kg$^{-1}$) from this study are similar to the 0.52–2.72 g kg$^{-1}$ found by Akagi et al. (2011) for different biomass burning emissions. Low EFs for particulate $Cl^-$, $NO_3^-$, $SO_4^{2-}$, and $NH_4^+$ were also reported by Pokhrel et al. (2021) for African biomass burning emissions.
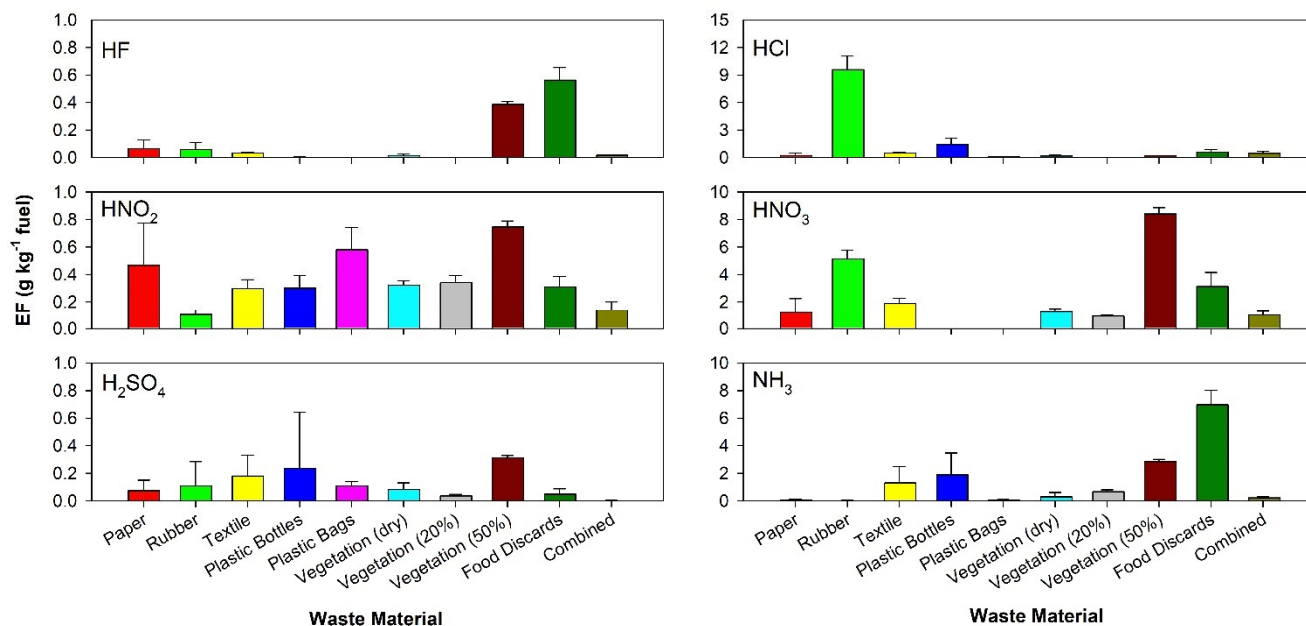
**Figure 5: Emission factors for acidic and alkali gases.**
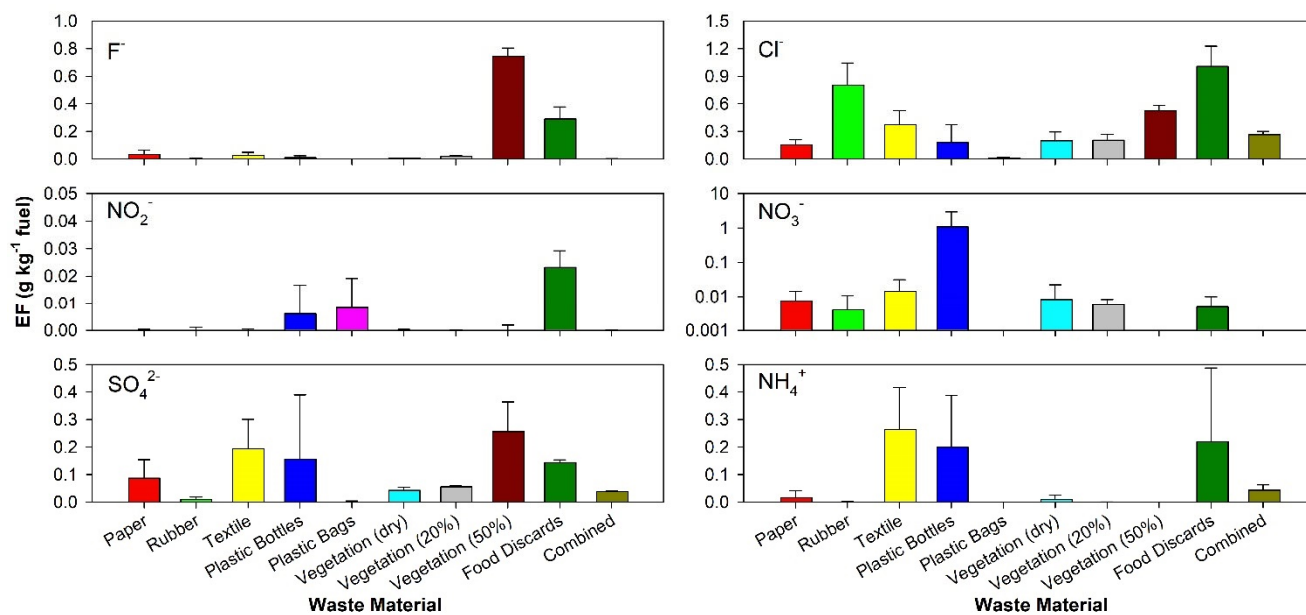
295     **Figure 6: Emission factors for ionic particulate species corresponding to the acidic and alkali gases.**

### 3.4 Non-polar Organic Compounds

The abundances (Figure 7~~Figure 7~~) and EFs (Figure S7) for organic groups differ among waste materials. Higher abundances of n-alkanes, phthalate, and PAHs are found for rubber and plastics (Figure 7~~Figure 7~~), consistent with elevated

EFs (Figure S8). Paper and textile emissions are dominated by n-alkanes. The high abundance of n-alkanes and phthalates in 300 solid waste burning is consistent with prior studies (Jayarathne et al., 2018; Simoneit et al., 2005).
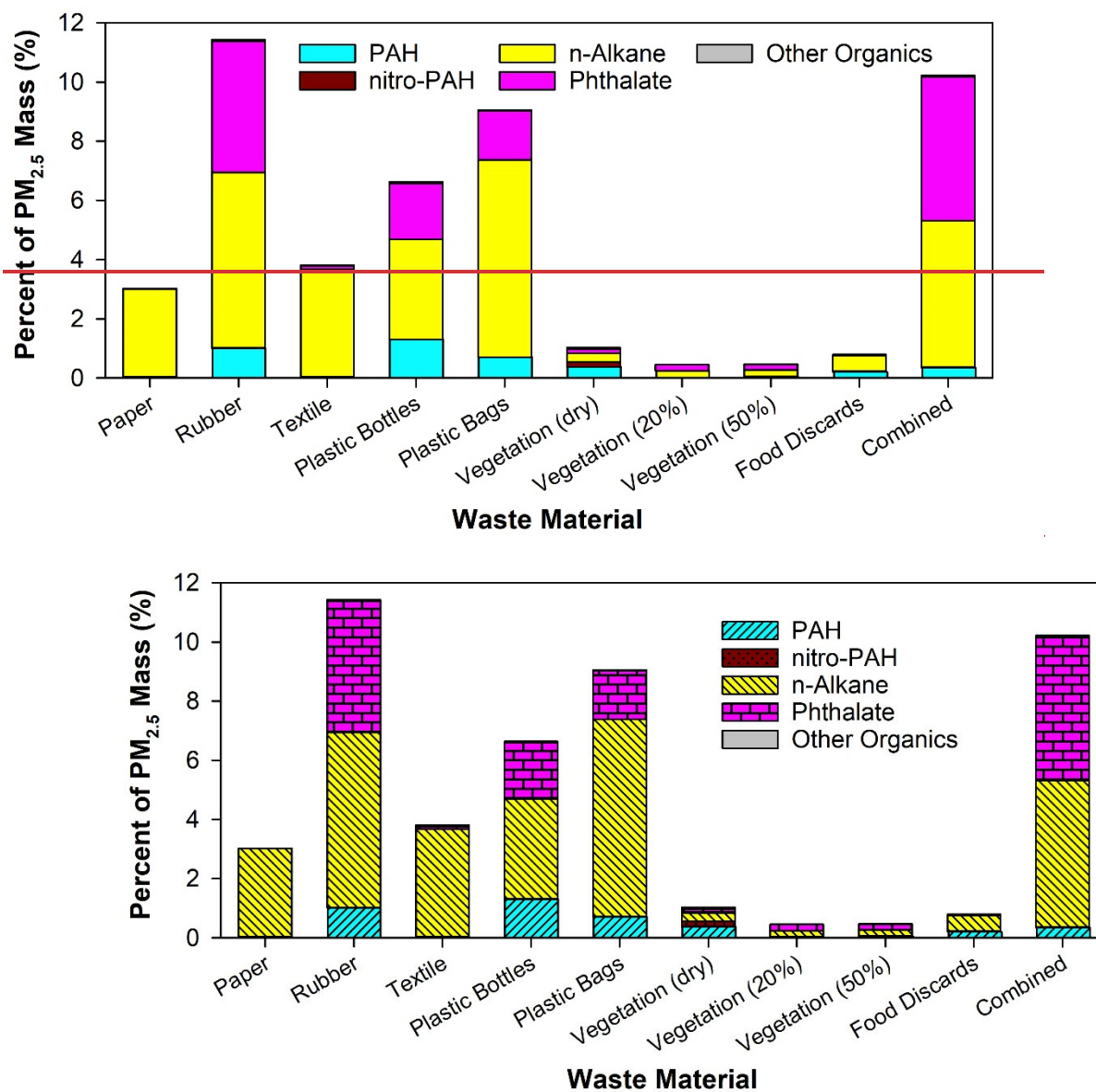
**Figure 7: Abundances for organic groups (% of PM₂.₅ mass).**

305 Figure 8~~Figure 8~~ shows the EFs for the most abundant PAHs including the U.S. EPA priority PAHs (Andersson and Achten, 2015). The PAH distribution shows similar patterns for rubber and plastic bottles/bags with dominant EFs and abundances (Figure S8) found for 5- and 6-ring PAHs (e.g., benzo[b]fluoranthene, benzo[j+k]fluoranthene, and indeno[1,2,3-cd]pyrene), although the relative abundances for rubber differ from those for plastic bottles and bags. Simoneit et al. (2005)

also reported that benzo[j+k]fluoranthene (0.02–0.036% of $PM_{10}$ mass) and indeno[1,2,3-cd]pyrene (0.01–0.024% of $PM_{10}$ mass) were the most abundant PAHs from plastics combustion. However, their abundances were an order of magnitude lower than the abundances found in this study (0.1–0.3% of $PM_{2.5}$ mass for both PAH species). Paper and textiles consist mostly of 4-ring PAHs, with high EFs for fluoranthene, pyrene, benzo[a]anthracene, and benzo[c]phenanthrene. The PAH EFs for textile were about twice those for paper. Vegetation and food discards burning emitted a wide range of PAHs, and the EFs varied significantly with moisture content.

PAH EFs from this study and those reported in the literature are compared in Table 1. Note that PAH compounds measured in different studies may be different. The PAH EF for paper from this study ($0.051 \pm 0.001$ g $kg^{-1}$) is in the same range as that reported by Wu et al. (2021), but is over an order of magnitude higher than those by Park et al. (2013) and Hoffer et al. (2020). Hoffer et al. (2020) also reported much lower PAH EFs for rubber but similar EFs for textile as compared to this study. The plastic bottle PAH EF from this study is over an order of magnitude higher than the other studies while the plastic bag and vegetation PAH EFs from this study are consistent with several other studies (Jayarathne et al., 2018; Hoffer et al., 2020; Wu et al., 2021; Andreae, 2019). However, the EFs for food discards are over 10 times higher than those for vegetation. The combined waste PAH EF from this study ($0.024 \pm 0.010$ g $kg^{-1}$) is close to that for recycled waste ($0.0235$–$0.0244$ g $kg^{-1}$) by Lemieux (1997) and dry mixed waste (0.015 g $kg^{-1}$) by Jayarathne et al. (2018). These EFs are lower than those reported for non-recycled waste (Lemieux, 1997) and damp mixed waste (Jayarathne et al., 2018).
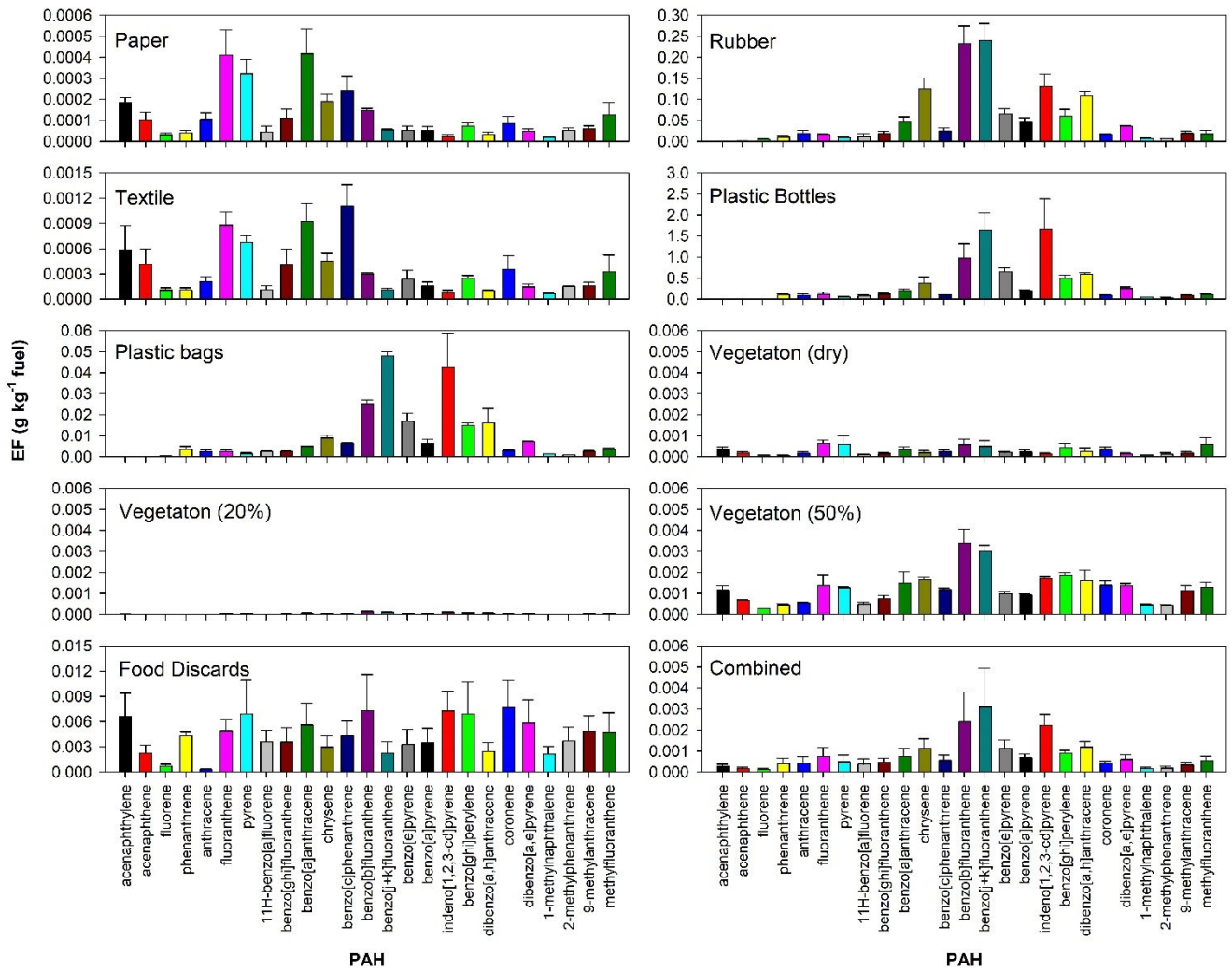
**Figure 8: Emission factors for PAHs.**

PAH diagnostic ratios have been used to infer PAH sources (U.S. DOT, 2022; Ravindra et al., 2008; Harner et al., 2018); however, not many ratios have been reported for MSW burning emissions (James et al., 2023). Table S3 lists several common PAH diagnostic ratios from this study. While there are similarities among different materials, some distinct ratios can be observed. For example, plastic bottles and bags have significantly ($p<0.05$) higher benzo[e]pyrene/benzo[a]pyrene and indeno[1,2,3-c,d]pyrene/benzo[g,h,i]perylene ratios; however, they had much lower emissions of retene, which is a biomass burning emission tracer, than other materials.

Figure 9~~Figure 9~~ and Figure S9 show that 2-nitrobuphenyl is the most abundant nitro-PAH for most MSW. Plastic bottles had the highest nitro-PAH EFs, followed by food discards and rubber. The dry vegetation had higher EFs than the moisture fuels.
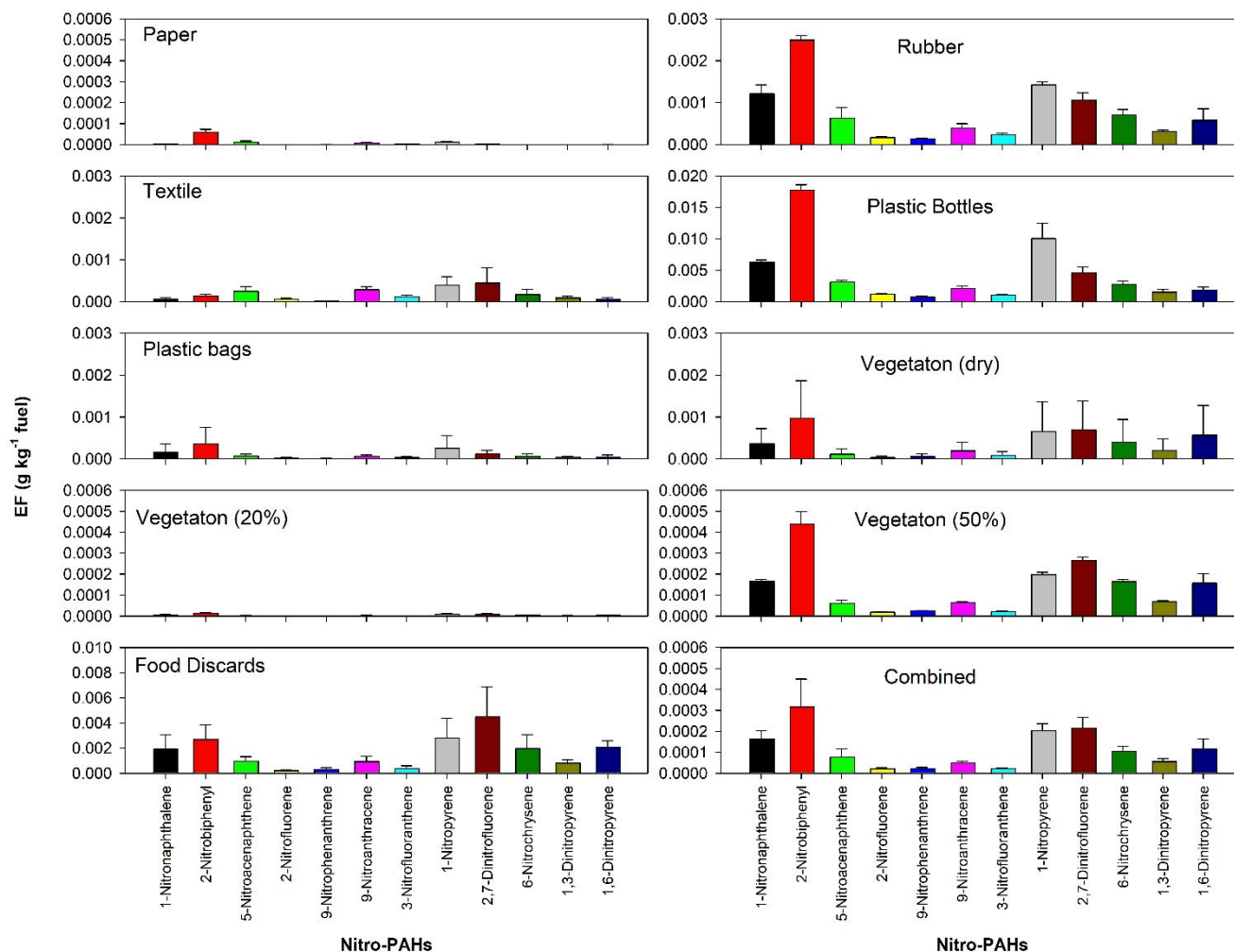
**Figure 9: Emission factors for nitro-PAHs.**

The cancer risks of PAHs and nitro-PAHs are often estimated using the equivalents of benzo(a)pyrene (BaP$_{eq}$), one of the most potent PAHs with known carcinogenic characteristics. The toxic equivalent factor (TEF) for BaP is set to 1 and other PAHs and nitro-PAHs are assigned a TEF value by comparing their relative toxicity to that of BaP (ATSDR, 2022; Samburova et al., 2017; Moradi et al., 2022). For PAHs, dibenzo[a,h]anthracene has the highest TEF of 2.4, followed by BaP, benzo[e]pyrene, and dibenzo[a,e]pyrene with a TEF of 1.0 (ATSDR, 2022; Samburova et al., 2017). For nitro-PAHs, 6-nitrochrysene and 1,6-dinitropyrene have the highest TEF of 10 (ATSDR, 2022). The EFs for BaP$_{eq}$ (BaP toxicity equivalent) were calculated from the sums of the products of the EF and TEF of individual PAHs and nitro-PAHs. Figure 10Figure 10 shows that plastic bottles, rubber, and plastic bags had the highest PAH EFs for BaP$_{eq}$, while plastic bottles, food discards, and rubber had the highest nitro-PAH EFs for BaP$_{eq}$, consistent with their high EFs for PAHs and nitro-PAHs. The PAH BaP$_{eq}$ EFs for paper ($0.00032 \pm 0.00010$ g kg$^{-1}$) and textile ($0.0010 \pm 0.0003$ g kg$^{-1}$) are in similar ranges with those reported by

Hoffer et al. (2020): $0.00016 \pm 0.00012$ g kg$^{-1}$ for paper and $0.0016 \pm 0.0020$ g kg$^{-1}$ for textile. However, the PAH BaP$_{eq}$ EFs for rubber ($0.47 \pm 0.06$ g kg$^{-1}$), plastic bags ($0.47 \pm 0.06$ g kg$^{-1}$), and plastic bottles ($3.0 \pm 0.4$ g kg$^{-1}$) were over an order of magnitude higher than the tire and plastics ($0.001$–$0.02$ g kg$^{-1}$) reported by Hoffer et al. (2020). These differences are likely caused by the more efficient oxidation by co-combustion of solid waste with charcoal in the Hoffer et al. (2020) tests and more PAH species were measured and included in the BaP$_{eq}$ calculation in this study.
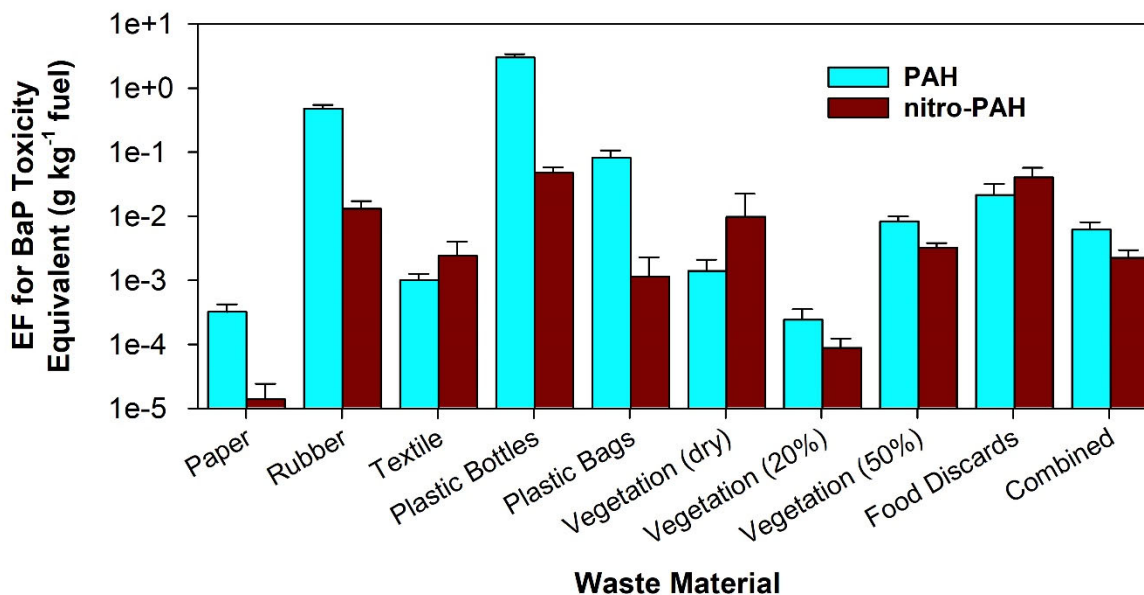
**Figure 10: Emission factors for total PAHs and nitro-PAHs expressed in benzo[a]pyrene (BaP) toxicity equivalent.**

Abundances and EFs for n-alkanes are shown in Figure S10 and Fig. 11, respectively. The most striking preference of odd alkanes over even alkanes was observed for the dry vegetation emissions, with a carbon preference index (CPI; the ratio of the sums of odd to even carbon numbers) of $6.01 \pm 0.47$, consistent with literature findings (Rogge et al., 1993; Noblet et al., 2021; Caumo et al., 2020). The higher than unity CPI is due to biogenic wax emissions. The EFs for 50% moisture vegetation were over an order of magnitude higher than those of dry and 20% moisture vegetation samples. However, the odd n-alkane preference was lost in emissions from moist vegetation, with CPI values of $0.63 \pm 0.01$ and $0.75 \pm 0.03$ for vegetation with 20% and 50% moisture contents, respectively. Paper, textile, and food discard emissions also showed preference for odd n-alkanes, with CPIs of $1.80 \pm 0.10$, $2.39 \pm 0.04$ and $2.53 \pm 0.21$, respectively. Plastic bottles had the highest EFs for n-alkanes, with C30-C32 having the highest EFs. Synthetic rubber and plastic bags had the second and third highest EFs for n-alkanes.
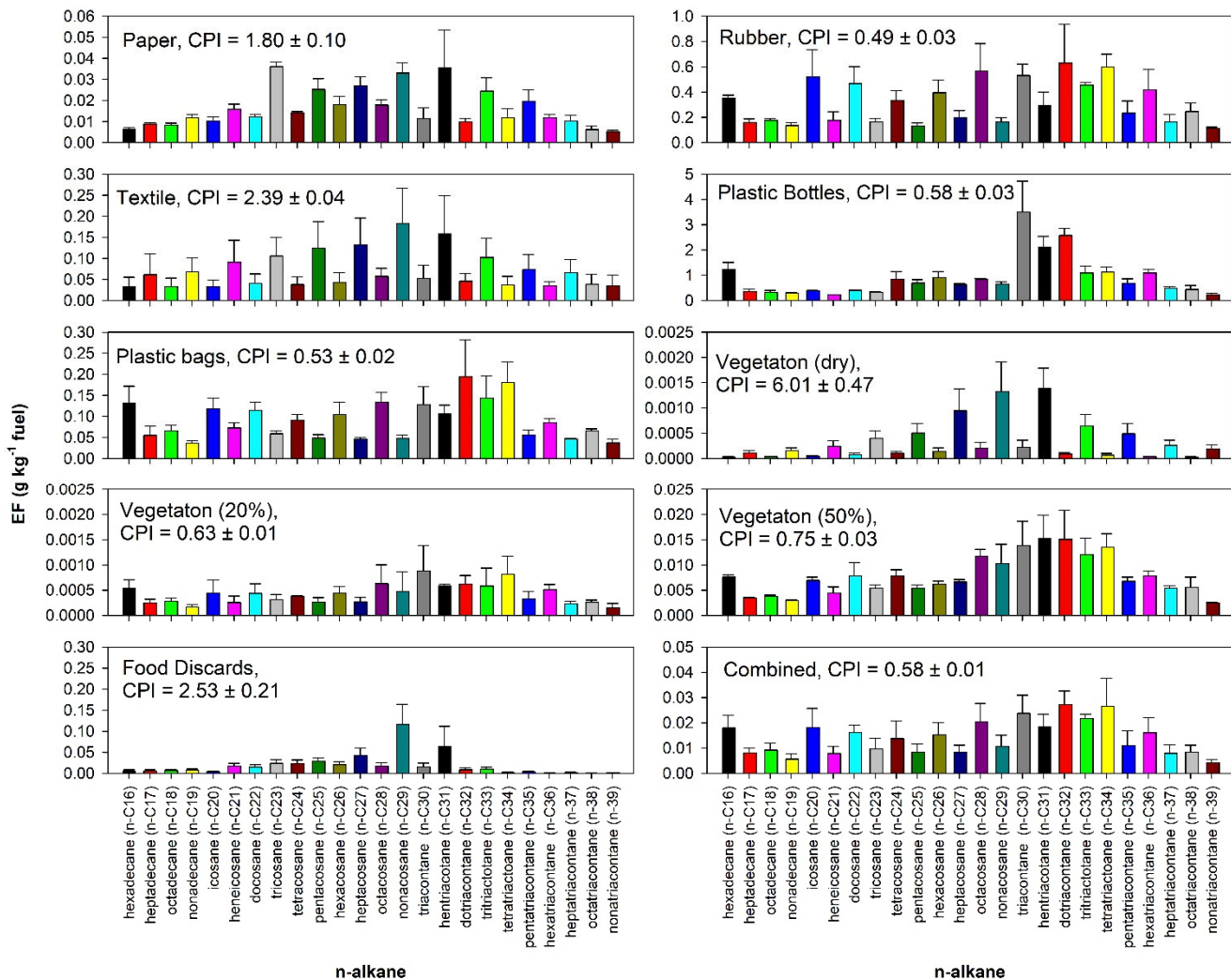
**Figure 11: Emission factors for n-alkanes.**

The CPIs for plastic bottles and bags, rubber, and combined waste material were less than 0.6, indicating combustion of petroleum products (Rogge et al., 1993). Jayarathne et al. (2018) reported CPIs of 0.6–1.1 for mixed waste, similar to the combined materials (0.58 ± 0.01) in this study. Simoneit et al. (2005) reported strong preferences for even carbon number n-alkanes (CPI = 0.1–0.47) for plastic extracts, but the preference decreased (CPI = 0.68–0.98) in the plastic burning smoke due to thermal cracking. These values are slightly higher but close to those for plastic bottles (0.58 ± 0.03) and plastic bags (0.53 ± 0.02). The carbon number maxima ($C_{max}$) are C30 and C32 for plastic bottles and C32 and C34 for plastic bags, consistent with the values reported by Simoneit et al. (2005).

Phthalates can irreversibly disrupt the endocrine system, metabolism, and multiple organs (Wang and Qian, 2021; Simoneit et al., 2005). Bis(2-ethylhexyl)phthalate (DEHP), one of the most common phthalates, was designated by the U.S.

Environmental Protection Agency (EPA) as a probable human carcinogen (Miao et al., 2017). EFs (Fig. 12) and percent PM$_{2.5}$
375   abundance (Figure S11) for phthalates are highest for plastic bottles and bags, rubber, and combined materials, consistent with
phthalates' use as plasticizing agents (Chien et al., 2003). Butyl benzyl phthalate (BBP), DEHP, and di-n-octyl phthalate
(DnBP) were the phthalate species with the highest EFs for all waste materials. Rubber had higher abundances of DnBP than
plastic bottles or bags. Phthalate EFs from 50% moisture vegetations are over an order of magnitude higher than the drier
vegetation samples, while paper had the lowest phthalate EFs.
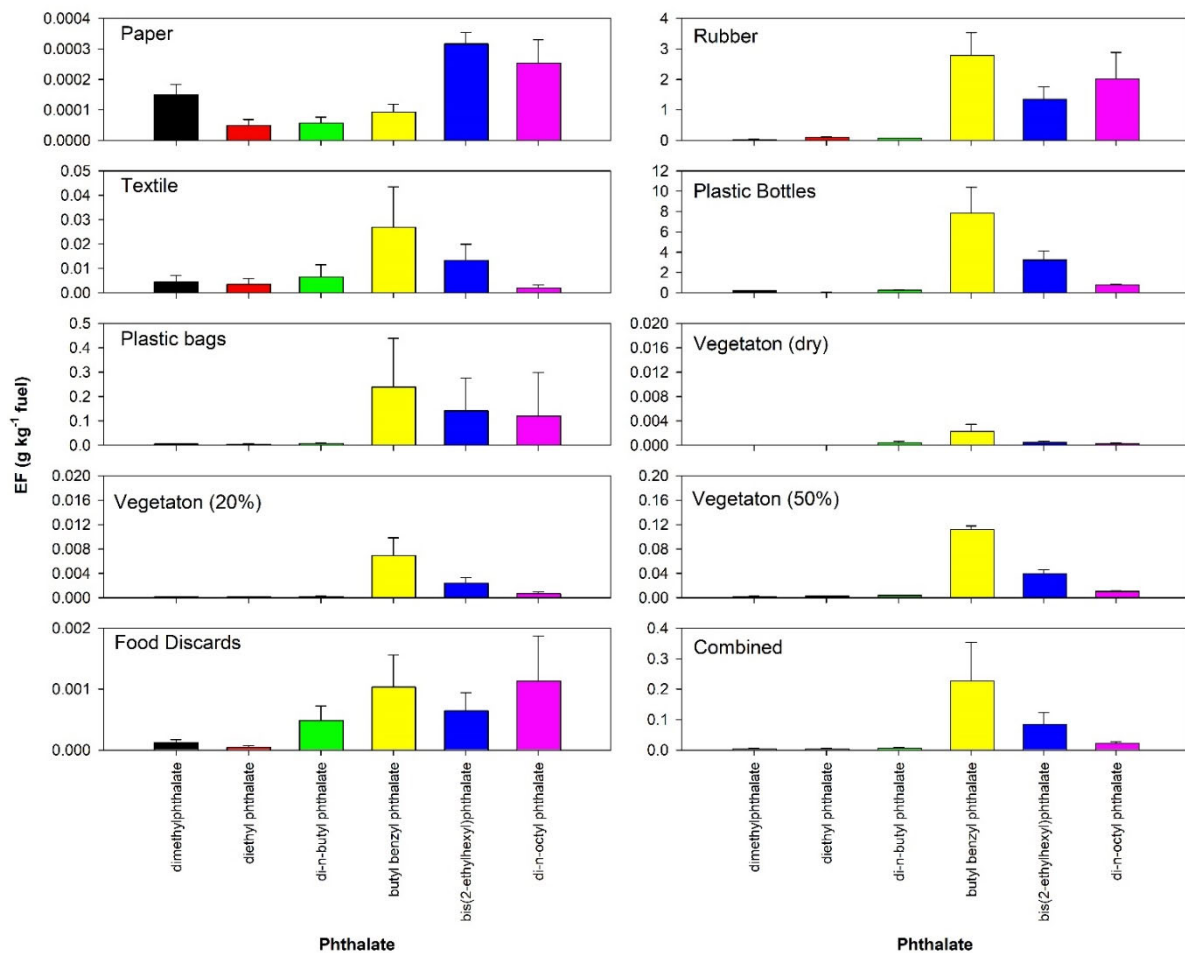
380

**Figure 12: Emission factors for phthalates.**

### 3.5 Summary of Chemical Characteristics and Emission Factors

Table 2 summarizes the key chemical characteristics of gases and PM$_{2.5}$ emitted from waste burning. These features can
serve as signatures of emission sources in source apportionment studies. OM was the most abundant component (>50% of
385   PM$_{2.5}$ mass) for all waste materials, and EC was more abundant in the flaming fuels, including plastic bags, combined fuels,
textile, and dry vegetation. The sum of the lower-temperature OC1 and OC2 components exceeded 20% for most fuels, except

for plastic bags and combined fuels which had the highest sums of EC1 and EC2 (53–70%). Cl was the most abundant element in $PM_{2.5}$ from all waste materials. Vegetation samples had higher abundances of K and $K^+$, confirming their use as biomass burning markers. Paper and textile non-polar organic emissions were dominated by n-alkanes. They had similar PAH distributions with abundant 4-ring PAHs (e.g., fluoranthene, pyrene, benzo[a]anthracene, and benzo[c]phenanthrene). Rubber, plastic bottles, and plastic bag emissions have high abundances of PAHs, n-alkanes, and phthalates, with abundant 5- and 6-ring PAHs (e.g., benzo[b]fluoranthene, benzo[j+k]fluoranthene, and indeno[1,2,3-cd]pyrene). Dry vegetation emissions produced approximately 10-fold higher PAH abundances than moist vegetation fuels, with a strong preference for odd n-alkanes and a CPI of $6.01 \pm 0.47$. In contrast, rubber, plastic bottles and bags showed preference to even n-alkanes, with CPI values less than 0.6. Rubber, plastic bottles and bags, and combined materials had the highest abundance of phthalates, while dry vegetation burning had the highest abundance of nitro-PAHs.

In term of EFs, Cl had the highest EFs among all elements measured by XRF. Rubber had the highest EFs for particulate Cl and S as well as gaseous HCl due to its most abundant Cl and S in the fuel. Rubber also had the highest EFs for HAP elements (Cd, Sb, and Pb), while 50% moisture vegetation had the highest EFs for Cr, Co, Ni, and Se. Food discards and 50% moisture vegetation had the highest EFs for HF, $NH_3$, and particulate $F^-$. The phthalates with the highest EFs are BBP, DEHP, and DnBP. Plastic bottles had the highest EFs for nitro-PAHs, followed by food discards and rubber. Among all measured nitro-PAHs, 2-nitrobiphenyl had the highest EFs for most waste materials.

**4 Conclusions and Discussion**

This study provides detailed chemical speciation of filter samples collected from laboratory combustion of ten municipal solid waste (MSW) materials, representing open burning of household waste in South Africa. Source profiles and emission factors were calculated. The key conclusions are:

(1) Source profiles representative of local emission sources are critical for accurate source apportionment (Watson et al., 2016). This study expands conventional elements, ions, and carbon fractions to include non-polar organic compounds such as PAHs, nitro-PAHs, alkanes and alkenes, and phthalates. The additional chemical speciation allows improvement in source attributions of open waste burning in South Africa and other regions in the world.

(2) Emission factors derived from the combustion of local materials that represent community-generated solid waste improve the accuracy of emission estimates. Emissions from open burning of MSW is under-studied for local, national, and global emission inventories (Wiedinmyer et al., 2014) with dearth of measurements for waste combustion (Rabaji, 2019; Kwatala et al., 2019). This study contributes to the air quality management and research communities by providing experimentally determined EFs for different waste material categories specific to South Africa. These localized EFs can be used to estimate the emission reductions for SASOL's WCI program and to improve MSW open burning emission inventories for South Africa and other countries.

**Table 2: Summary of chemical abundance characteristics of emissions from open burning of different waste materials.**

| Material | Major Composition | Carbon | Elements | Inorganic Ions | Non-polar Organics |
|---|---|---|---|---|---|
| Paper | Flaming, high EC; OM = 76%; EC = 6.5% | High OC3+OC4 = 18.6% | Metals from ink (e.g., Cu) | High $HNO_3$ (8.6%) | Dominated by n-alkanes (3%); similar PAH distribution as textile |
| Rubber | Smoldering, high OM; OM = 98%; EC = 0.2% | High OC1+OC2 = 70% | High Cl (1.1%) and Sb (0.05%) | High HCl (6.7%) | High abundances of PAHs (4.4%), n-alkanes (5.9%), and phthalate (4.4%); high even n-alkane preference (CPI = 0.49) |
| Textile | Flaming, high EC; OM = 86%; EC = 12.1% | High OC1+OC2 = 48% and EC1+EC2 = 20% | | High $NH_4^+$ (0.53%) | Dominated by n-alkanes (3.6%); similar PAH distribution as paper |
| Plastic bottle | Smoldering, high OM; OM = 98%; EC = 0.4% | High OC1+OC2 = 53% | Low elemental abundances | Low gaseous and particulate ions | High abundances of PAHs (1.3%), n-alkanes (3.4%), and phthalate (1.9%); high even n-alkane preference (CPI = 0.58) |
| Plastic bag | Flaming, highest EC; OM = 50%; EC = 49% | Low OC1+OC2 = 7.5% and highest EC2 = 63% | Low elemental abundances | Low gaseous and particulate ions | Highest abundance of n-alkane (6.7%), and high abundances of PAHs (0.7%) and phthalate (1.7%); high even n-alkane preference (CPI = 0.53) |
| Vegetation (dry) | Flaming, high EC and ions; OM = 80%; EC = 8.2%; ions: 9.9% | High OC3+OC4 = 29.6% and EC1 = 15.8% | Highest Cl (5.1%) and K (3.3%) | Highest $HNO_2$ (11%), $HNO_3$ (43%), Cl- (7.1%) | Low non-polar organic abundances; high odd n-alkane preference (CPI = 6); highest nitro-PAH abundances (0.17%) |
| Vegetation (20%) | Flaming, high ions; OM = 81%; EC = 4.2%; ions: 8.8% | High OC3+OC4 = 22.3% | High Cl (4.0%) and K (2.4%) | Highest $NH_3$ (17%) and $K^+$ (2.1%), and high $HNO_2$ (8%), $HNO_3$ (21%), and Cl- (5%) | Low non-polar organic abundances |
| Vegetation (50%) | Smoldering, high OM; OM = 81%; EC = 2.6% | High OC1+OC2 = 37% | Lower Cl and K than drier vegetations | Highest F- (0.85%) | Low non-polar organic abundances |
| Food discards | Smoldering, high OM; OM = 73%; EC = 0.8% | High OC1+OC2 = 38% | Low heavy metals | Similar to 50% moist vegetation | Low non-polar organic abundances |
| Combined | Flaming, high EC and ions; OM = 46%; EC = 47%; ions: 6% | Low OC1+OC2 = 15% and high EC1 + EC2 = 53% | Highest lead abundance (0.08%) | High $HNO_3$ (15%), HCl (6.8%), and Cl- (4.1%) | High abundances of n-alkanes (5%), and phthalate (4.9%) |

420

(3) EFs for chemical species provide additional information to assess potential health risks associated with exposure to open burning emissions. The established chemical database can be used for risk assessment to further demonstrate emission reductions for many air toxics (e.g., hazardous gases, heavy metals, and PAHs) beyond criteria pollutants by reducing open waste burning. The EFs for $CO_2$ and EC are also useful for evaluating the climate impacts from MSW open burning.

(4) The EFs determined for nine individual waste categories and the combined waste category offer flexibility in calculating emissions. When the weight composition is known for open burn piles, emissions of chemical species can be calculated by summing those from individual categories; otherwise, the EFs for the combined categories can be used. EFs for $PM_{2.5}$ from this study are within the ranges reported in the literature. This study fills a data gap, particularly for speciated profiles and EFs from burning many waste materials, such as paper, leather/rubber, textiles, and food discards.

(5) Results were obtained from laboratory tests simulating real-world conditions. However, the differences in fuel mixtures, packing structure, moisture content, burn conditions, dilution, and aging between laboratory and field conditions will cause differences in chemical compositions and EFs (Hodshire et al., 2019). The EFs might need to be adjusted when real-world burning conditions differ significantly from the test conditions used in this study.

**Data availability.** The source profile and emission factor data are available at: Wang, X., 2023, "Data for: Air Pollutant Emissions from Open Burning of Household Solid Waste from South Africa", https://doi.org/10.7910/DVN/QTV9YW, Harvard Dataverse, V1. Additional data is available upon request.

**Author contributions.** XW, JCC, and JGW designed the study; HF conducted the combustion experiments; SSHH conducted organic speciation; XW performed the data analyses and prepared the original paper draft; WC and ASMDV provided waste materials and resources; all authors reviewed and edited the paper.

**Competing interests.** None.

**Financial support.** This research was partially funded by SASOL (grant no. 2000751484) and partially by the Desert Research Institute internal funding.

**References**

Akagi, S. K., Yokelson, R. J., Wiedinmyer, C., Alvarado, M. J., Reid, J. S., Karl, T., Crounse, J. D., and Wennberg, P. O.: Emission factors for open and domestic biomass burning for use in atmospheric models, Atmos. Chem. Phys., 11, 4039-4072, https://doi.org/10.5194/acp-11-4039-2011, 2011.

450 Andersson, J. T. and Achten, C.: Time to Say Goodbye to the 16 EPA PAHs? Toward an Up-to-Date Use of PACs for Environmental Purposes, Polycyclic Aromat. Compd., 35, 330-354, https://doi.org/10.1080/10406638.2014.991042, 2015.

Andreae, M. O.: Emission of trace gases and aerosols from biomass burning – an updated assessment, Atmos. Chem. Phys., 19, 8523-8546, 10.5194/acp-19-8523-2019, 2019.

455 ATSDR: Guidance for Calculating Benzo(a)pyrene Equivalents for Cancer Evaluations of Polycyclic Aromatic Hydrocarbons Agency for Toxic Substances and Disease Registry (ATSDR), U.S. Department of Health and Human Services, Public Health Service, Atlanta, GA, 2022.

Bond, T. C., Doherty, S. J., Fahey, D. W., Forster, P. M., Berntsen, T., DeAngelo, B. J., Flanner, M. G., Ghan, S., Kärcher, B., Koch, D., Kinne, S., Kondo, Y., Quinn, P. K., Sarofim, M. C., Schultz, M. G., Schulz, M., Venkataraman, C., Zhang, H.,
460 Zhang, S., Bellouin, N., Guttikunda, S. K., Hopke, P. K., Jacobson, M. Z., Kaiser, J. W., Klimont, Z., Lohmann, U., Schwarz, J. P., Shindell, D., Storelvmo, T., Warren, S. G., and Zender, C. S.: Bounding the role of black carbon in the climate system: A scientific assessment, Journal of Geophysical Research: Atmospheres, 118, 5380-5552, https://doi.org/10.1002/jgrd.50171, 2013.

Bulto, T. W.: Impact of Open Burning Refuse on Air Quality: In the Case of "Hidar Sitaten" at Addis Ababa, Ethiopia,
465 Environmental Health Insights, 14, 1-11, https://doi.org/10.1177/1178630220943204, 2020.

Caumo, S., Bruns, R. E., and Vasconcellos, P. C.: Variation of the Distribution of Atmospheric n-Alkanes Emitted by Different Fuels' Combustion, Atmosphere, 11, 643, https://doi.org/10.3390/atmos11060643, 2020.

Chen, L.-W. A., Chow, J. C., Wang, X. L., Robles, J. A., Sumlin, B., Lowenthal, D. H., Zimmermann, R., and Watson, J. G.: Multi-wavelength optical measurement to enhance thermal/optical analysis for carbonaceous aerosol, Atmos. Meas. Tech.,
470 8, 451-461, https://doi.org/10.5194/amt-8-451-2015, 2015.

Cheng, K., Hao, W., Wang, Y., Yi, P., Zhang, J., and Ji, W.: Understanding the emission pattern and source contribution of hazardous air pollutants from open burning of municipal solid waste in China, Environ. Pollut., 263, 114417, https://doi.org/10.1016/j.envpol.2020.114417, 2020.

Chien, Y.-C., Ton, S., Lee, M.-H., Chia, T., Shu, H.-Y., and Wu, Y.-S.: Assessment of occupational health hazards in scrap-
475 tire shredding facilities, Sci. Total Environ., 309, 35-46, https://doi.org/10.1016/S0048-9697(03)00009-3, 2003.

Chow, J. C. and Watson, J. G.: Chemical analyses of particle filter deposits, in: Aerosols Handbook : Measurement, Dosimetry, and Health Effects, 2 ed., edited by: Ruzer, L., and Harley, N. H., CRC Press/Taylor & Francis, New York, NY, 179-204, 2013.

Chow, J. C. and Watson, J. G.: Enhanced ion chromatographic speciation of water-soluble $PM_{2.5}$ to improve aerosol source
480 apportionment, Aerosol Science and Engineering, 1, 7-24, doi:10.1007/s41810-017-0002-4, 2017.

Chow, J. C., Watson, J. G., Edgerton, S. A., and Vega, E.: Chemical composition of PM2.5 and PM10 in Mexico City during winter 1997, Sci. Total Environ., 287, 177-201, https://doi.org/10.1016/S0048-9697(01)00982-2, 2002.

Chow, J. C., Chen, L.-W. A., Wang, X. L., Green, M. C., and Watson, J. G.: Improved estimation of PM2.5 brown carbon contributions to filter light attenuation, Particuology, 56, 1-9, https://doi.org/10.1016/j.partic.2021.01.001, 2021.

485 Chow, J. C., Lowenthal, D. H., Chen, L.-W. A., Wang, X. L., and Watson, J. G.: Mass reconstruction methods for $PM_{2.5}$: a review, Air Quality, Atmosphere & Health, 8, 243-263, https://doi.org/10.1007/s11869-015-0338-3, 2015a.

Chow, J. C., Watson, J. G., Chen, L.-W. A., Chang, M. C. O., Robinson, N. F., Trimble, D., and Kohl, S.: The IMPROVE_A temperature protocol for thermal/optical carbon analysis: maintaining consistency with a long-term database, Journal of the Air & Waste Management Association, 57, 1014-1023, 2007.

490 Chow, J. C., Wang, X. L., Sumlin, B. J., Gronstal, S. B., Chen, L.-W. A., Hurbain, M. J., Zimmermann, R., and Watson, J. G.: Optical Calibration and Equivalence of a Multiwavelength Thermal/Optical Carbon Analyzer, Aerosol Air Qual. Res., 15, 1145-1159, https://doi.org/10.4209/aaqr.2015.02.0106, 2015b.

Chow, J. C., Watson, J. G., Green, M. C., Wang, X. L., Chen, L.-W. A., Trimble, D. L., Cropper, P. M., Kohl, S. D., and Gronstal, S. B.: Separation of brown carbon from black carbon for IMPROVE and Chemical Speciation Network PM2.5
495 samples, J. Air Waste Manage. Assoc., 68, 494-510, https://doi.org/10.1080/10962247.2018.1426653, 2018.

Christian, T. J., Yokelson, R. J., Cárdenas, B., Molina, L. T., Engling, G., and Hsu, S. C.: Trace gas and particle emissions from domestic and industrial biofuel use and garbage burning in central Mexico, Atmos. Chem. Phys., 10, 565-584, https://doi.org/10.5194/acp-10-565-2010, 2010.

Cook, E. and Velis, C.: Global review on safer end of engineered life, Royal Academy of Engineering, London, UK, https://doi.org/10.5518/100/58, 2021.

Cronjé, N., Van Der Merwe, I., and Müller, I.-M.: Household food waste: A case study in Kimberley, South Africa, Journal of Consumer Sciences, 46, 1-9, 2018.

Das, B., Bhave, P. V., Sapkota, A., and Byanju, R. M.: Estimating emissions from open burning of municipal solid waste in municipalities of Nepal, Waste Manage. (Oxford), 79, 481-490, https://doi.org/10.1016/j.wasman.2018.08.013, 2018.

Eldering, A., Solomon, P. A., Salmon, L. G., Fall, T., and Cass, G. R.: Hydrochloric acid: A regional perspective on concentrations and formation in the atmosphere of Southern California, Atmospheric Environment. Part A. General Topics, 25, 2091-2102, https://doi.org/10.1016/0960-1686(91)90086-M, 1991.

Gordon, J. N. D., Bilsback, K. R., Fiddler, M. N., Pokhrel, R. P., Fischer, E. V., Pierce, J. R., and Bililign, S.: The Effects of Trash, Residential Biofuel, and Open Biomass Burning Emissions on Local and Transported PM2.5 and Its Attributed Mortality in Africa, GeoHealth, 7, e2022GH000673, https://doi.org/10.1029/2022GH000673, 2023.

Harner, T., Rauert, C., Muir, D., Schuster, J. K., Hsu, Y.-M., Zhang, L., Marson, G., Watson, J. G., Ahad, J., Cho, S., Jariyasopit, N., Kirk, J., Korosi, J., Landis, M. S., Martin, J. W., Zhang, Y., Fernie, K., Wentworth, G. R., Wnorowski, A., Dabek, E., Charland, J.-P., Pauli, B., Wania, F., Galarneau, E., Cheng, I., Makar, P., Whaley, C., Chow, J. C., and Wang, X. L.: Air synthesis review: polycyclic aromatic compounds in the oil sands region, Environmental Reviews, 26, 430-468, https://doi.org/10.1139/er-2018-0039, 2018.

Ho, S. S. H. and Yu, J. Z.: In-injection port thermal desorption and subsequent gas chromatography-mass spectrometric analysis of polycyclic aromatic hydrocarbons and *n*-alkanes in atmospheric aerosol samples, J. Chromatogr. A, 1059, 121-129, https://doi.org/10.1016/j.chroma.2004.10.013, 2004.

Ho, S. S. H., Chow, J. C., Watson, J. G., Ng, L. P. T., Kwok, Y., Ho, K. F., and Cao, J. J.: Precautions for in-injection port thermal desorption-gas chromatography/mass spectrometry (TD-GC/MS) as applied to aerosol filter samples, Atmos. Environ., 45, 1491-1496, 10.1016/j.atmosenv.2010.12.038, 2011.

Ho, S. S. H., Yu, J. Z., Chow, J. C., Zielinska, B., Watson, J. G., Sit, E. H. L., and Schauer, J. J.: Evaluation of an in-injection port thermal desorption-gas chromatography/mass spectrometry method for analysis of non-polar organic compounds in ambient aerosol samples, J. Chromatogr. A, 1200, 217-227, https://doi.org/10.1016/j.chroma.2008.05.056, 2008.

Hodshire, A. L., Akherati, A., Alvarado, M. J., Brown-Steiner, B., Jathar, S. H., Jimenez, J. L., Kreidenweis, S. M., Lonsdale, C. R., Onasch, T. B., Ortega, A. M., and Pierce, J. R.: Aging Effects on Biomass Burning Aerosol Mass and Composition: A Critical Review of Field and Laboratory Studies, Environ. Sci. Technol., 53, 10007-10022, 10.1021/acs.est.9b02588, 2019.

Hoffer, A., Jancsek-Turóczi, B., Tóth, Á., Kiss, G., Naghiu, A., Levei, E. A., Marmureanu, L., Machon, A., and Gelencsér, A.: Emission factors for PM10 and polycyclic aromatic hydrocarbons (PAHs) from illegal burning of different types of municipal waste in households, Atmos. Chem. Phys., 20, 16135-16144, https://doi.org/10.5194/acp-20-16135-2020, 2020.

IPCC: 2006 IPCC guidelines for national greenhouse gas inventories, National Greenhouse Gas Inventories Programme Japan; Intergovernmental Panel on Climate Change (IPCC): Geneva, Switzerland, 2006.

IPCC: Climate change 2013: The physical science basis. Working Group I Contribution to the Fifth Assessment Report of the Intergovernmental Panel on Climate Change, Cambridge University Press Cambridge, UK, and New York2013.

James, B. D., Reddy, C. M., Hahn, M. E., Nelson, R. K., de Vos, A., Aluwihare, L. I., Wade, T. L., Knap, A. H., and Bera, G.: Fire and Oil Led to Complex Mixtures of PAHs on Burnt and Unburnt Plastic during the M/V X-Press Pearl Disaster, ACS Environmental Au, https://doi.org/10.1021/acsenvironau.3c00011, 2023.

Jayarathne, T., Stockwell, C. E., Yokelson, R. J., Nakao, S., and Stone, E. A.: Emissions of Fine Particle Fluoride from Biomass Burning, Environ. Sci. Technol., 48, 12636-12644, https://doi.org/10.1021/es502933j, 2014.

Jayarathne, T., Stockwell, C. E., Bhave, P. V., Praveen, P. S., Rathnayake, C. M., Islam, M. R., Panday, A. K., Adhikari, S., Maharjan, R., Goetz, J. D., DeCarlo, P. F., Saikawa, E., Yokelson, R. J., and Stone, E. A.: Nepal Ambient Monitoring and Source Testing Experiment (NAMaSTE): emissions of particulate matter from wood- and dung-fueled cooking fires, garbage and crop residue burning, brick kilns, and other sources, Atmos. Chem. Phys., 18, 2259-2286, https://doi.org/10.5194/acp-18-2259-2018, 2018.

Kelly, F. J. and Fussell, J. C.: Size, source and chemical composition as determinants of toxicity attributable to ambient particulate matter, Atmos. Environ., 60, 504-526, https://doi.org/10.1016/j.atmosenv.2012.06.039, 2012.

Kleeman, M. J., Schauer, J. J., and Cass, G. R.: Size and composition distribution of fine particulate matter emitted from motor vehicles, Environ. Sci. Technol., 34, 1132-1142, 10.1021/es981276y, 2000.

550 Kodros, J. K., Wiedinmyer, C., Ford, B., Cucinotta, R., Gan, R., Magzamen, S., and Pierce, J. R.: Global burden of mortalities due to chronic exposure to ambient PM 2.5 from open combustion of domestic waste, Environ. Res. Lett., 11, 124022, https://doi.org/10.1088/1748-9326/11/12/124022, 2016.

Krecl, P., de Lima, C. H., Dal Bosco, T. C., Targino, A. C., Hashimoto, E. M., and Oukawa, G. Y.: Open waste burning causes fast and sharp changes in particulate concentrations in peripheral neighborhoods, Sci. Total Environ., 765, 142736,
555 https://doi.org/10.1016/j.scitotenv.2020.142736, 2021.

Kwatala, N., Naidoo, M., Naidoo, S., and Garland, R. M.: Estimated emissions of domestic waste burning in South Africa, 2019 Conference of the National Association for Clean Air, Western Cape, October 3-4, 2019,

Lal, R. M., Nagpure, A. S., Luo, L., Tripathi, S. N., Ramaswami, A., Bergin, M. H., and Russell, A. G.: Municipal solid waste and dung cake burning: discoloring the Taj Mahal and human health impacts in Agra, Environ. Res. Lett., 11, 104009,
560 https://doi.org/10.1088/1748-9326/11/10/104009, 2016.

Lemieux, P. M.: Evaluation of emissions from the open burning of household waste in barrels - Volume 1. Technical Report, National Risk Management Research Laboratory, US Environmental Protection Agency, Cincinnati, OHEPA-600/R-97-134a, 1997.

Lemieux, P. M.: Evaluation of emissions from the open burning of household waste in barrels - Project Summary, National
565 Risk Management Research Laboratory, US Environmental Protection Agency, Cincinnati, OH EPA/600/SR-97/134, 1998.

Lemieux, P. M., Lutes, C. C., and Santoianni, D. A.: Emissions of organic air toxics from open burning: a comprehensive review, Prog. Energy Combust. Sci., 30, 1-32, https://doi.org/10.1016/j.pecs.2003.08.001, 2004.

Lighty, J. S., Veranth, J. M., and Sarofim, A. F.: Combustion Aerosols: Factors Governing Their Size and Composition and
570 Implications to Human Health, J. Air Waste Manage. Assoc., 50, 1565-1618, https://doi.org/10.1080/10473289.2000.10464197, 2000.

Malm, W., Sisler, J., Huffman, D., Eldred, R., and Cahill, T.: Spatial and seasonal trends in particle concentration and optical extinction in the United States, J. Geophys. Res., 99, 1347-1370, https://doi.org/10.1029/93JD02916, 1994.

Martuzzi, M., Mitis, F., and Forastiere, F.: Inequalities, inequities, environmental justice in waste management and health,
575 European Journal of Public Health, 20, 21-26, https://doi.org/10.1093/eurpub/ckp216, 2010.

Miao, Y., Wang, R., Lu, C., Zhao, J., and Deng, Q.: Lifetime cancer risk assessment for inhalation exposure to di(2-ethylhexyl) phthalate (DEHP), Environ. Sci. Pollut. Res., 24, 312-320, https://doi.org/10.1007/s11356-016-7797-4, 2017.

Moradi, M., Hung, H., Li, J., Park, R., Shin, C., Alexandrou, N., Iqbal, M. A., Takhar, M., Chan, A., and Brook, J. R.: Assessment of Alkylated and Unsubstituted Polycyclic Aromatic Hydrocarbons in Air in Urban and Semi-Urban Areas
580 in Toronto, Canada, Environ. Sci. Technol., 56, 2959-2967, https://doi.org/10.1021/acs.est.1c04299, 2022.

Murray, C. J., Aravkin, A. Y., Zheng, P., Abbafati, C., Abbas, K. M., Abbasi-Kangevari, M., Abd-Allah, F., Abdelalim, A., Abdollahi, M., and Abdollahpour, I.: Global burden of 87 risk factors in 204 countries and territories, 1990–2019: a systematic analysis for the Global Burden of Disease Study 2019, The lancet, 396, 1223-1249, https://doi.org/10.1016/S0140-6736(20)30752-2, 2020.

585 Nagpure, A. S., Ramaswami, A., and Russell, A.: Characterizing the Spatial and Temporal Patterns of Open Burning of Municipal Solid Waste (MSW) in Indian Cities, Environ. Sci. Technol., 49, 12904-12912, https://doi.org/10.1021/acs.est.5b03243, 2015.

Noblet, C., Besombes, J.-L., Lemire, M., Pin, M., Jaffrezo, J.-L., Favez, O., Aujay-Plouzeau, R., Dermigny, A., Karoski, N., Van Elsuve, D., Dubois, P., Collet, S., Lestremau, F., and Albinet, A.: Emission factors and chemical characterization of
590 particulate emissions from garden green waste burning, Sci. Total Environ., 798, 149367, https://doi.org/10.1016/j.scitotenv.2021.149367, 2021.

Okedere, O. B., Olalekan, A. P., Fakinle, B. S., Elehinafe, F. B., Odunlami, O. A., and Sonibare, J. A.: Urban air pollution from the open burning of municipal solid waste, Environ. Qual. Manage., 28, 67-74, https://doi.org/10.1002/tqem.21633, 2019.

595 Oleniacz, R., Drzewiecki, W., Gorzelnik, T., Grzesik, K., Kozakiewicz, R., Kowalewski, Z., and Kossakowska, K.: Assessment of the impact of waste fires on air quality and atmospheric aerosol optical depth: A case study in Poland, Energy Reports, 9, 16-38, https://doi.org/10.1016/j.egyr.2023.03.087, 2023.

Pani, S. K., Chantara, S., Khamkaew, C., Lee, C.-T., and Lin, N.-H.: Biomass burning in the northern peninsular Southeast Asia: Aerosol chemical profile and potential exposure, Atmos. Res., 224, 180-195, https://doi.org/10.1016/j.atmosres.2019.03.031, 2019.

Park, Y. K., Kim, W., and Jo, Y. M.: Release of Harmful Air Pollutants from Open Burning of Domestic Municipal Solid Wastes in a Metropolitan Area of Korea, Aerosol Air Qual. Res., 13, 1365-1372, https://doi.org/10.4209/aaqr.2012.10.0272, 2013.

Pokhrel, R. P., Gordon, J., Fiddler, M. N., and Bililign, S.: Determination of Emission Factors of Pollutants From Biomass Burning of African Fuels in Laboratory Measurements, Journal of Geophysical Research: Atmospheres, 126, e2021JD034731, https://doi.org/10.1029/2021JD034731, 2021.

Pöschl, U.: Aerosol particle analysis: challenges and progress, Anal. Bioanal.Chem., 375, 30-32, https://doi.org/10.1007/s00216-002-1611-5, 2003.

Rabaji, O. P.: Waste dumping in Sharpeville (Emfuleni Municipality): an investigation of the characteristics and the potential impacts on air quality, M.S., Environmental Management, North-West University, Potchefstroom, South Africa, 2019.

Ramadan, B. S., Rachman, I., Ikhlas, N., Kurniawan, S. B., Miftahadi, M. F., and Matsumoto, T.: A comprehensive review of domestic-open waste burning: recent trends, methodology comparison, and factors assessment, J. Mater. Cycles Waste Manage., 24, 1633-1647, https://doi.org/10.1007/s10163-022-01430-9, 2022.

Ravindra, K., Sokhi, R., and Van Grieken, R.: Atmospheric polycyclic aromatic hydrocarbons: Source attribution, emission factors and regulation, Atmos. Environ., 42, 2895-2921, https://doi.org/10.1016/j.atmosenv.2007.12.010, 2008.

Reff, A., Bhave, P. V., Simon, H., Pace, T. G., Pouliot, G. A., Mobley, J. D., and Houyoux, M.: Emissions Inventory of $PM_{2.5}$ Trace Elements across the United States, Environ. Sci. Technol., 43, 5790-5796, https://doi.org/10.1021/es802930x, 2009.

Reid, J. S., Koppmann, R., Eck, T. F., and Eleuterio, D. P.: A review of biomass burning emissions part II: intensive physical properties of biomass burning particles, Atmos. Chem. Phys., 5, 799-825, 10.5194/acp-5-799-2005, 2005.

Reyna-Bensusan, N., Wilson, D. C., and Smith, S. R.: Uncontrolled burning of solid waste by households in Mexico is a significant contributor to climate change in the country, Environ. Res., 163, 280-288, https://doi.org/10.1016/j.envres.2018.01.042, 2018.

Rogge, W. F., Hildemann, L. M., Mazurek, M. A., Cass, G. R., and Simoneit, B. R. T.: Sources of fine organic aerosol. 2. Noncatalyst and catalyst-equipped automobiles and heavy-duty diesel trucks, Environ. Sci. Technol., 27, 636-651, 1993.

Samburova, V., Zielinska, B., and Khlystov, A.: Do 16 Polycyclic Aromatic Hydrocarbons Represent PAH Air Toxicity?, Toxics, 5, https://doi.org/10.3390/toxics5030017, 2017.

Sharma, G., Annadate, S., and Sinha, B.: Will open waste burning become India's largest air pollution source?, Environ. Pollut., 292, 118310, https://doi.org/10.1016/j.envpol.2021.118310, 2022.

Simon, H., Beck, L., Bhave, P. V., Divita, F., Hsu, Y., Luecken, D., Mobley, J. D., Pouliot, G. A., Reff, A., Sarwar, G., and Strum, M.: The development and uses of EPA's SPECIATE database, Atmospheric Pollution Research, 1, 196-206, http://dx.doi.org/10.5094/APR.2010.026, 2010.

Simoneit, B. R. T., Medeiros, P. M., and Didyk, B. M.: Combustion Products of Plastics as Indicators for Refuse Burning in the Atmosphere, Environ. Sci. Technol., 39, 6961-6970, https://doi.org/10.1021/es050767x, 2005.

Stockwell, C. E.: Advanced measurements of undersampled globally significant biomass burning sources, Chemistry, The University of Montana, Missoula, MT, 2016.

Stockwell, C. E., Christian, T. J., Goetz, J. D., Jayarathne, T., Bhave, P. V., Praveen, P. S., Adhikari, S., Maharjan, R., DeCarlo, P. F., Stone, E. A., Saikawa, E., Blake, D. R., Simpson, I. J., Yokelson, R. J., and Panday, A. K.: Nepal Ambient Monitoring and Source Testing Experiment (NAMaSTE): emissions of trace gases and light-absorbing carbon from wood and dung cooking fires, garbage and crop residue burning, brick kilns, and other sources, Atmos. Chem. Phys., 16, 11043-11081, https://doi.org/10.5194/acp-16-11043-2016, 2016.

Sturges, W. T. and Harrison, R. M.: The use of nylon filters to collect HCl: efficiencies, interferences and ambient concentrations, Atmos. Environ.(1967), 23, 1987-1996, https://doi.org/10.1016/0004-6981(89)90525-8, 1989.

Turpin, B. J. and Lim, H.-J.: Species Contributions to $PM_{2.5}$ Mass Concentrations: Revisiting Common Assumptions for Estimating Organic Mass, Aerosol Sci. Technol., 35, 602 - 610, 2001.

U.S. DOT: Safety Advisory Notice for the Disposal and Recycling of Lithium Batteries in Commercial Transportation, Pipeline and Hazardous Materials Safety Administration, Office of Hazardous Materials Safety, U.S. Department of Transportation, Washington, DC, 2022.

U.S. EPA: Compilation of Air Pollutant Emissions Factors AP-42, Fifth Edition Section 2.5 Open Burning, U.S. Environmental Protection Agency, Research Triangle Park, NCEPA AP-42, 1992.

650 U.S. EPA: Quality Assurance Guidance Document - Quality Assurance Project Plan: $PM_{2.5}$ Chemical Speciation Sampling at Trends, NCore, Supplemental and Tribal Sites, Ambient Air Monitoring Group, Air Quality Assessment Division, US EPA, Office of Air Quality Planning and Standards, Research Triangle Park, North Carolina, 2012.

U.S. EPA: Initial List of Hazardous Air Pollutants with Modifications, Air Toxics Assessment Group, U.S. Environmental Protection Agency Research Triangle Park, NC, 2020.

655 U.S. EPA: 2020 National Emissions Inventory Technical Support Document: Waste Disposal – Open Burning – Residential Household Waste, Air Quality Assessment Division, Office of Air Quality Planning and Standards, U.S. Environmental Protection Agency (U.S. EPA) Research Triangle Park, NC, 2023.

Valavanidis, A., Iliopoulos, N., Gotsis, G., and Fiotakis, K.: Persistent free radicals, heavy metals and PAHs generated in particulate soot emissions and residue ash from controlled combustion of common types of plastic, J. Hazard. Mater., 156,

660 277-284, https://doi.org/10.1016/j.jhazmat.2007.12.019, 2008.

Velis, C. A. and Cook, E.: Mismanagement of Plastic Waste through Open Burning with Emphasis on the Global South: A Systematic Review of Risks to Occupational and Public Health, Environ. Sci. Technol., 55, 7186-7207, https://doi.org/10.1021/acs.est.0c08536, 2021.

Wang, X. L., Firouzkouhi, H., Chow, J. C., Watson, J. G., Ho, S. S. H., Carter, W., and De Vos, A. S. M.: Characterization of

665 gas and particle emissions from open burning of household solid waste from South Africa, Atmos. Chem. Phys., 23, 8921–8937, https://doi.org/10.5194/acp-23-8921-2023, 2023.

Wang, Y. and Qian, H.: Phthalates and Their Impacts on Human Health, Healthcare (Basel, Switzerland), 9, https://doi.org/10.3390/healthcare9050603, 2021.

Wasson, S. J., Linak, W. P., Gullett, B. K., King, C. J., Touati, A., Huggins, F. E., Chen, Y., Shah, N., and Huffman, G. P.:

670 Emissions of Chromium, Copper, Arsenic, and PCDDs/Fs from Open Burning of CCA-Treated Wood, Environ. Sci. Technol., 39, 8865-8876, https://doi.org/10.1021/es050891g, 2005.

Watson, J. G.: Visibility: Science and regulation, J. Air Waste Manage. Assoc., 52, 628-713, 2002.

Watson, J. G., Chow, J. C., and Frazier, C. A.: X-ray fluorescence analysis of ambient air samples, in: Elemental Analysis of Airborne Particles, Vol. 1, edited by: Landsberger, S., and Creatchman, M., Advances in Environmental, Industrial and

675 Process Control Technologies, Gordon and Breach Science, Amsterdam, The Netherlands, 67-96, 1999.

Watson, J. G., Chow, J. C., Engling, G., Chen, L.-W. A., and Wang, X. L.: Source apportionment: Principles and methods, in: Airborne Particulate Matter: Sources, Atmospheric Processes and Health, edited by: Harrison, R. M., Royal Society of Chemistry, London, UK, 72-125, 2016.

Watson, J. G., Tropp, R. J., Kohl, S. D., Wang, X. L., and Chow, J. C.: Filter processing and gravimetric analysis for suspended

680 particulate matter samples, Aerosol Science and Engineering, 1, 193-205, 2017.

Wiedinmyer, C., Yokelson, R. J., and Gullett, B. K.: Global Emissions of Trace Gases, Particulate Matter, and Hazardous Air Pollutants from Open Burning of Domestic Waste, Environ. Sci. Technol., 48, 9523-9530, https://doi.org/10.1021/es502250z, 2014.

Williams, M., Gower, R., Green, J., Whitebread, E., Lenkiewicz, Z., and Schröder, P.: No time to waste: Tackling the plastic

685 pollution crisis before it's too late, Tearfund, London, UK, 2019.

Wu, D., Li, Q., Shang, X., Liang, Y., Ding, X., Sun, H., Li, S., Wang, S., Chen, Y., and Chen, J.: Commodity plastic burning as a source of inhaled toxic aerosols, J. Hazard. Mater., 416, 125820, https://doi.org/10.1016/j.jhazmat.2021.125820, 2021.

Zięba-Palus, J. and Trzcińska, B. M.: Establishing of Chemical Composition of Printing Ink, Journal of Forensic Sciences, 56,

690 819-821, https://doi.org/10.1111/j.1556-4029.2011.01734.x, 2011.

# Chemically Speciated Air Pollutant Emissions from Open Burning of Household Solid Waste from South Africa

Xiaoliang Wang[1], Hatef Firouzkouhi[1], Judith C. Chow[1], John G. Watson[1], Steven Sai Hang Ho[1],
Warren Carter[2], Alexandra S.M. De Vos[2]

[1] Division of Atmospheric Sciences, Desert Research Institute, Reno, NV 89512, U.S.A.
[2] SASOL Research and Technology, Sasolburg, South Africa

*Correspondence to*: Xiaoliang Wang (xiaoliang.wang@dri.edu)

## S1. PM$_{2.5}$ Mass Closure

Mass closure, a comparison of the reconstructed mass and sum of measured species with gravimetric mass, is an indicator of the data quality. It also provides information about key chemical composition and potential sources of PM$_{2.5}$ (Chow et al., 2015a).

15 Sum of measured species should be less than or equal to the corresponding gravimetric PM$_{2.5}$ mass concentrations because species such as oxygen (O) and hydrogen (H) are not measured. The U.S. Environmental Protection Agency (EPA) Quality Assurance Guidance for PM$_{2.5}$ Chemical Speciation suggests that the ratio of sum of species over gravimetric mass should be within the range of 0.60–1.32 (U.S. EPA, 2012). This sum includes chemicals quantified on the Teflon-membrane and quartz-fiber filters without double counting. Measured concentrations do not account for
20 unmeasured O associated with metal oxides in minerals, unmeasured anions and cations, or H, N, and O associated with organic carbon. Figure S1a shows that the sum of species accounts 73% of PM$_{2.5}$, which is within the U.S. EPA limit.

Mass reconstruction consists of five major categories, including organic matter (OM = OC × $f_{OM/OC}$~~multiplier~~), elemental carbon (EC), ions, minerals, and other species (Chow et al., 2015a; Watson et al., 2016). ~~A multiplier of 1.4~~
25 ~~is used to convert OC to OM.~~ Ions include ammonium (NH$_4^+$), sodium (Na$^+$), magnesium (Mg$^{2+}$), potassium (K$^+$), calcium (Ca$^{2+}$), fluoride (F$^-$), chloride (Cl$^-$), nitrite (NO$_2^-$), nitrate (NO$_3^-$), and sulfate (SO$_4^{2-}$) by IC (Chow and Watson, 2017). Minerals are estimated as 2.2×Al + 2.49×Si + 1.63×Ca + 2.42×Fe + 1.94×Ti, following the IMPROVE formula (Chow et al., 2015a; Malm et al., 1994). "Other species" include the measured species not included in the major components without double counting.

30 The multiplier ($f_{OM/OC}$) for converting OC to OM varies with the composition of OM, ranging from 1.2 for fresh vehicle engine emissions (Kleeman et al., 2000) and fresh urban aerosols (Chow et al., 2002) to 2.6 for aged aerosols (Turpin and Lim, 2001). A value of 1.4 has been most commonly used for urban aerosols, and a value of 1.8 is used

for more aged non-urban aerosols (Chow et al., 2015a). Reid et al. (2005) found the $f_{OM/OC}$ to be ~1.5 for fresh biomass burning smoke. Assuming that all species are measured and analytical uncertainties are negligible, $f_{OM/OC}$ values for

35    different materials are estimated from mass closure as (Pani et al., 2019):

$$f_{OM/OC} = \frac{PM_{2.5} - EC - Ions - Minerals - Others}{OC} \tag{S1}$$

Table S1 shows that $f_{OM/OC}$ varies from 1.22 for dry vegetation to 1.87 for food discards, with smoldering materials (except rubber) having higher values than flaming fuels, indicating more oxygens in organic aerosols from smoldering combustions. The overall average $f_{OM/OC}$ value for all test conditions is 1.4, which is used to convert OC to OM in

40    mass reconstruction.

Figure S1b compares reconstructed with gravimetric masses showing a linear regression slope of 0.99. Note that some data points have reconstructed masses higher or lower than gravimetric mass, likely due to uncertainties in the estimation of OM and minerals as well as potential positive and negative sampling artifacts. The differences between gravimetric and reconstructed masses are referred to as unidentified species. Because the mass closure has ratios close

45    to unity based on both sum of species and reconstructed mass, the chemical analysis of major $PM_{2.5}$ constituents (i.e., gravimetric mass, carbon, ions, and elements) are of high quality.

**Table S1: Measured organic matter (OM) to organic carbon (OC) ratio $f_{OM/OC}$.**

| Material | OM/OC |
|---|---|
| Paper | 1.66 ± 0.16 |
| Rubber | 1.27 ± 0.07 |
| Textile | 1.36 ± 0.28 |
| Plastic (Bottles) | 1.42 ± 0.02 |
| Plastic (Bags) | 1.66 ± 0.60 |
| Vegetation (0%) | 1.22 ± 0.11 |
| Vegetation (20%) | 1.38 ± 0.15 |
| Vegetation (50%) | 1.63 ± 0.12 |
| Food Discards | 1.87 ± 0.09 |
| Combined | 1.40 ± 0.21 |

(a)                                                                                          (b)
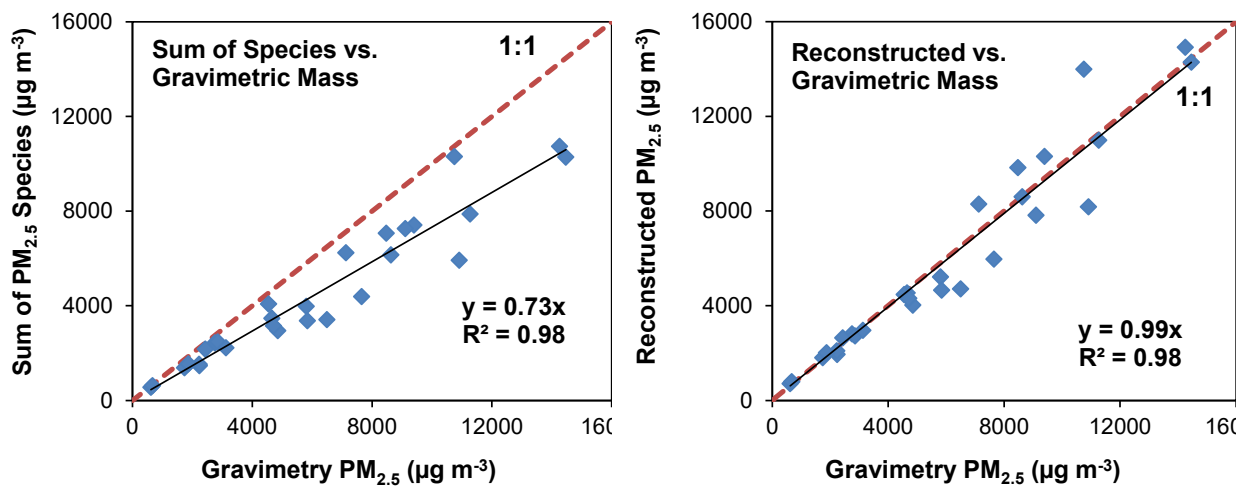
50 **Figure S1: Comparison of: (a) sum of species and (b) reconstructed mass with gravimetric mass of PM₂.₅.**

## S2. Supplementary Tables

55

**Table S2~~1~~: Comparison of heavy metal emission factors (mg kg$^{-1}$ fuel) between this study and those from other published measurements.**

| Element | Cr | Ni | Cu | Zn | Cd | Pb |
|---|---|---|---|---|---|---|
| Paper | | | | | | |
| **This study** | **0.22 ± 0.34** | **0.00 ± 0.06** | **4.30 ± 2.79** | **0.91 ± 0.74** | **0.00 ± 0.77** | **1.70 ± 1.30** |
| (Park et al., 2013) | 0.33–0.38 | 0.20–0.26 | 0.07–0.22 | 0–18.19 | 0.02–0.05 | 0–0.07 |
| (Cheng et al., 2020) | 0.43–0.69 | 0.54–0.74 | 6.17–6.96 | 1.20–2.09 | 0.27–0.37 | 1.83–1.99 |
| Plastics | | | | | | |
| **This study (bottle)** | **4.75 ± 1.91** | **0.00 ± 0.94** | **5.81 ± 9.72** | **0.27 ± 3.17** | **0.52 ± 12.42** | **12.53 ± 10.99** |
| **This study (bag)** | **0.26 ± 0.24** | **0.00 ± 0.07** | **3.36 ± 1.01** | **0.99 ± 0.40** | **0.00 ± 0.92** | **1.77 ± 0.88** |
| (Park et al., 2013) | 0.36–1.46 | 0.05–0.24 | 0.04–0.12 | 0–65.17 | 0.01–0.02 | 0.002–1.13 |
| (Cheng et al., 2020) | 0.49–0.80 | 0.48–0.62 | 7.02–8.0 | 1.66–3.73 | 0.28–0.45 | 1.14–1.33 |
| Vegetations | | | | | | |
| **This study (0%)** | **0.26 ± 0.45** | **0.00 ± 0.06** | **0.86 ± 0.75** | **0.41 ± 1.47** | **0.39 ± 0.58** | **0.50 ± 0.74** |
| **This study (20%)** | **0.64 ± 0.16** | **0.04 ± 0.08** | **0.35 ± 0.49** | **1.18 ± 3.37** | **0.00 ± 0.45** | **0.87 ± 0.48** |
| **This study (50%)** | **5.94 ± 1.33** | **0.24 ± 0.68** | **5.01 ± 3.50** | **2.13 ± 27.22** | **0.00 ± 3.63** | **8.37 ± 2.15** |
| (Park et al., 2013) | 0.14–0.46 | 0.07–0.50 | 0.05–0.18 | 2.69–15.65 | 0.01–0.19 | 0.05–0.10 |
| (Cheng et al., 2020) | 0.27–0.31 | 0.34–0.38 | 5.38–5.45 | 0.85–2.13 | 0.18–0.23 | 1.03–1.21 |
| Combined Materials | | | | | | |
| **This study** | **0.00 ± 0.06** | **0.00 ± 0.03** | **1.53 ± 0.30** | **0.56 ± 0.53** | **0.07 ± 0.41** | **5.59 ± 4.55** |
| (Lemieux, 1997) | 0.176–0.237 | 0.188–0.804 | 0.573–15.02 | 0.073–18.9 | 0.037–0.239 | 0.22–2.57 |
| (Christian et al., 2010) | | | 0.35–2.13 | 0.98–1.72 | 0.27–0.59 | 4.0–7.8 |
| (Park et al., 2013) | 0.53–1.02 | 0.15–0.66 | 0.04–0.08 | 13.29–14.16 | 0.01–0.02 | 0.01–0.05 |
| (Jayarathne et al., 2018) | | | 0.29 ± 0.07 | | 0.07 ± 0.15 | 4.2 ± 5.7 |
| (Cheng et al., 2020) | 0.41–0.62 | 0.46–0.53 | 6.55–6.84 | 1.06–2.44 | 0.27–0.35 | 1.12–1.25 |

60  **Table S32: PAH diagnostic ratios.**

| Diagnostic ratios | Paper | Rubber | Textile | Plastic (Bottles) | Plastic (Bags) | Vegetation (0%) | Vegetation (20%) | Vegetation (50%) | Food | Combined |
|---|---|---|---|---|---|---|---|---|---|---|
| FL/(FL+PYR) | 0.09 ± 0.03 | 0.39 ± 0.09 | 0.14 ± 0.02 | 0.18 ± 0.06 | 0.19 ± 0.05 | 0.12 ± 0.06 | 0.12 ± 0.02 | 0.18 ± 0.01 | 0.10 ± 0.03 | 0.20 ± 0.04 |
| PHE/ANT | 0.41 ± 0.05 | 0.52 ± 0.02 | 0.52 ± 0.03 | 1.10 ± 0.08 | 1.49 ± 0.53 | 0.36 ± 0.04 | 0.76 ± 0.11 | 0.82 ± 0.06 | 16.14 ± 3.15 | 0.93 ± 0.11 |
| ANT/(ANT+PHE) | 0.71 ± 0.03 | 0.66 ± 0.01 | 0.66 ± 0.01 | 0.48 ± 0.02 | 0.41 ± 0.08 | 0.74 ± 0.02 | 0.57 ± 0.03 | 0.55 ± 0.02 | 0.06 ± 0.01 | 0.52 ± 0.03 |
| FLA/PYR | 1.27 ± 0.19 | 1.98 ± 0.67 | 1.31 ± 0.21 | 2.22 ± 1.31 | 1.81 ± 0.48 | 1.21 ± 0.40 | 1.04 ± 0.11 | 1.09 ± 0.43 | 0.81 ± 0.29 | 1.57 ± 0.10 |
| FLA/(FLA+PYR) | 0.56 ± 0.04 | 0.65 ± 0.07 | 0.56 ± 0.04 | 0.66 ± 0.12 | 0.64 ± 0.06 | 0.54 ± 0.09 | 0.51 ± 0.03 | 0.51 ± 0.10 | 0.44 ± 0.10 | 0.61 ± 0.02 |
| BaA/CHR | 2.17 ± 0.23 | 0.36 ± 0.10 | 2.00 ± 0.19 | 0.61 ± 0.22 | 0.57 ± 0.09 | 1.91 ± 0.95 | 1.46 ± 0.45 | 0.92 ± 0.41 | 1.98 ± 0.88 | 0.65 ± 0.12 |
| BaA/(BaA+CHR) | 0.68 ± 0.02 | 0.26 ± 0.05 | 0.67 ± 0.02 | 0.37 ± 0.08 | 0.36 ± 0.04 | 0.63 ± 0.12 | 0.59 ± 0.07 | 0.47 ± 0.11 | 0.65 ± 0.10 | 0.39 ± 0.05 |
| PYR/BaP | 6.17 ± 0.79 | 0.19 ± 0.02 | 4.48 ± 1.30 | 0.26 ± 0.04 | 0.24 ± 0.08 | 2.50 ± 0.78 | 1.06 ± 0.15 | 1.39 ± 0.08 | 2.04 ± 0.56 | 0.67 ± 0.29 |
| BaP/(BaP+CHR) | 0.22 ± 0.07 | 0.27 ± 0.05 | 0.26 ± 0.05 | 0.37 ± 0.14 | 0.41 ± 0.06 | 0.56 ± 0.12 | 0.52 ± 0.10 | 0.36 ± 0.04 | 0.53 ± 0.09 | 0.39 ± 0.04 |
| BeP/BaP | 1.00 ± 0.07 | 1.48 ± 0.52 | 1.45 ± 0.25 | 3.23 ± 0.86 | 2.76 ± 0.51 | 0.85 ± 0.07 | 1.04 ± 0.12 | 1.07 ± 0.18 | 0.92 ± 0.07 | 1.63 ± 0.30 |
| BaP/BghiP | 0.72 ± 0.16 | 0.82 ± 0.32 | 0.62 ± 0.10 | 0.42 ± 0.12 | 0.43 ± 0.16 | 0.57 ± 0.13 | 0.56 ± 0.06 | 0.49 ± 0.03 | 0.51 ± 0.11 | 0.76 ± 0.14 |
| IcdP/BghiP | 0.29 ± 0.09 | 2.23 ± 0.47 | 0.28 ± 0.14 | 3.22 ± 1.03 | 2.86 ± 1.07 | 0.31 ± 0.08 | 1.04 ± 0.36 | 0.91 ± 0.11 | 1.15 ± 0.30 | 2.45 ± 0.48 |
| IcdP/(IcdP+BghiP) | 0.22 ± 0.05 | 0.69 ± 0.05 | 0.21 ± 0.09 | 0.75 ± 0.07 | 0.72 ± 0.09 | 0.23 ± 0.05 | 0.50 ± 0.09 | 0.48 ± 0.03 | 0.53 ± 0.07 | 0.71 ± 0.04 |
| RET/(RET+CHR) | 0.74 ± 0.08 | 0.00 ± 0.00 | 0.78 ± 0.07 | 0.00 ± 0.00 | 0.00 ± 0.00 | 0.55 ± 0.09 | 0.39 ± 0.09 | 0.31 ± 0.06 | 0.57 ± 0.04 | 0.21 ± 0.09 |

PAH abbreviations:
ANT: Anthracene          BaA: Benzo[a]anthracene      BaP: Benzo[a]pyrene      BeP: Benzo[e]pyrene
BghiP: Benzo[g,h,i]perylene   CHR: Chrysene            FL: Fluorene             FLA: Fluoranthene
65  IcdP: Indeno[1,2,3-c,d]pyrene   PHE: Phenanthrene        PYR: Pyrene              RET: retene

**S3. Supplementary Figures**
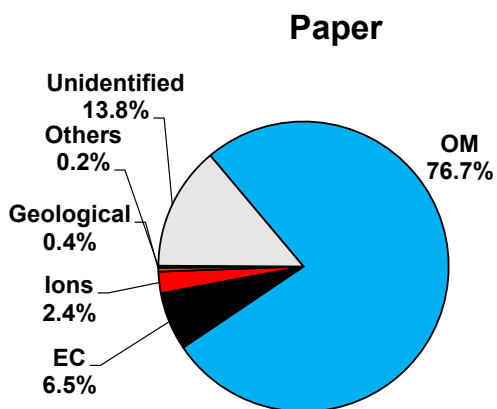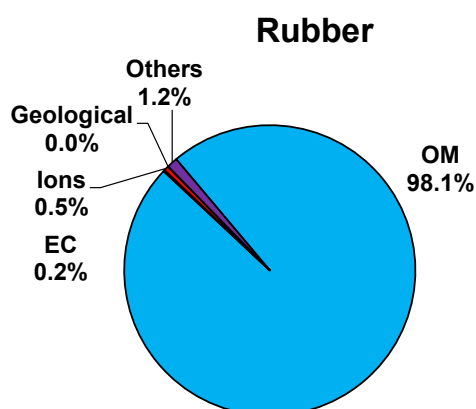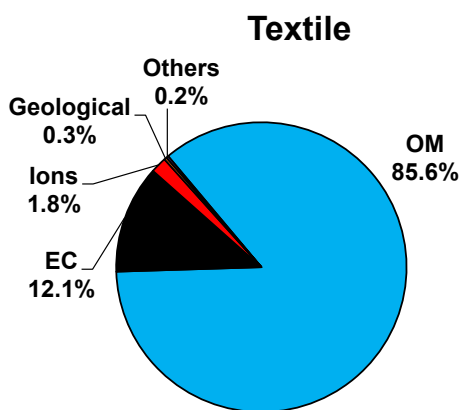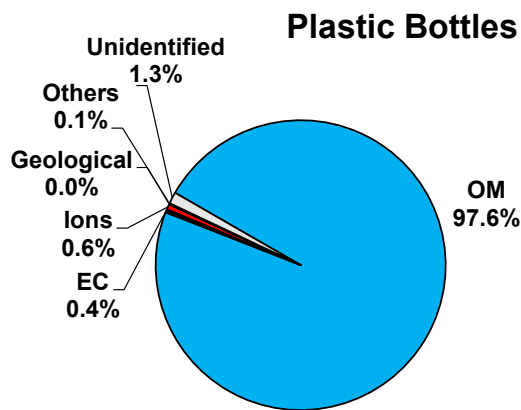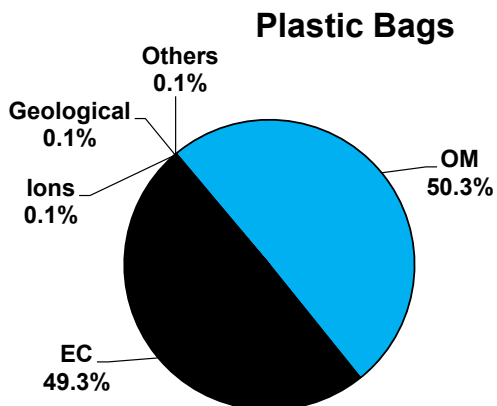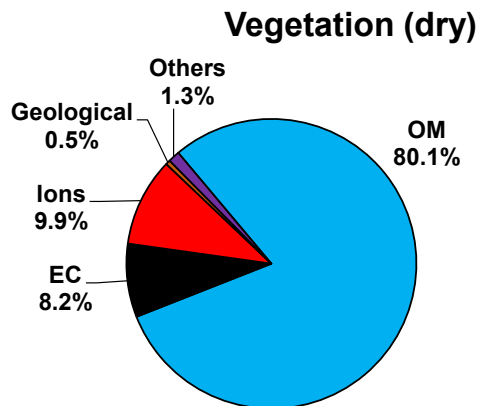
**Figure S2: Major chemical composition (% of PM$_{2.5}$ mass) for waste materials tested.**

g)

**Vegetation
(20% moisture)**

Others
4.4%

Geological
1.3%

Ions
8.8%

EC
4.2%

OM
81.4%

h)

**Vegetation
(50% moisture)**

Unidentified
12.8%

Others
1.6%

Geological
0.6%

Ions
1.9%

EC
2.6%

OM
80.5%

i)

**Food**

Unidentified
24.3%

Others
0.1%

Geological
0.0%

Ions
2.1%

EC
0.8%

OM
72.7%

j)

**Combined**

Others
0.3%

Geological
0.4%

Ions
6.0%

EC
47.1%

OM
46.2%
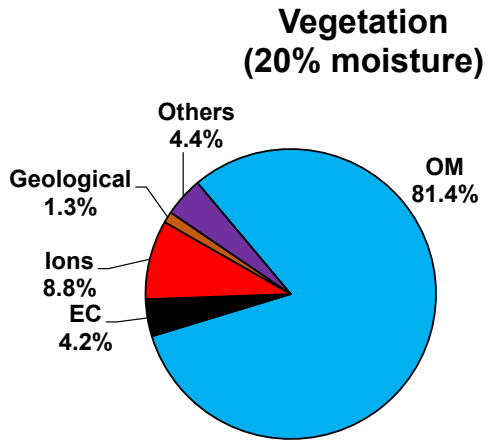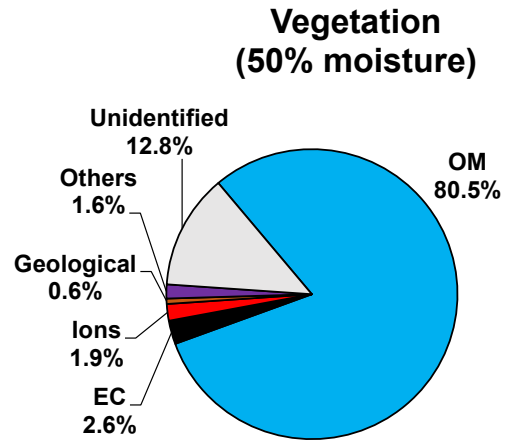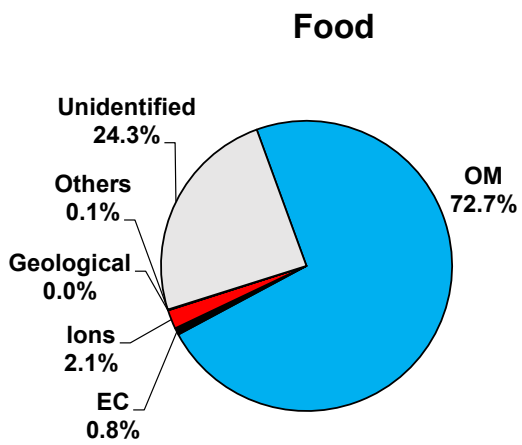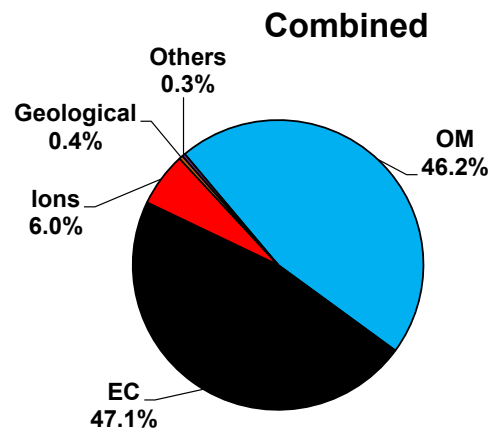
70

**Figure S2 continued.**
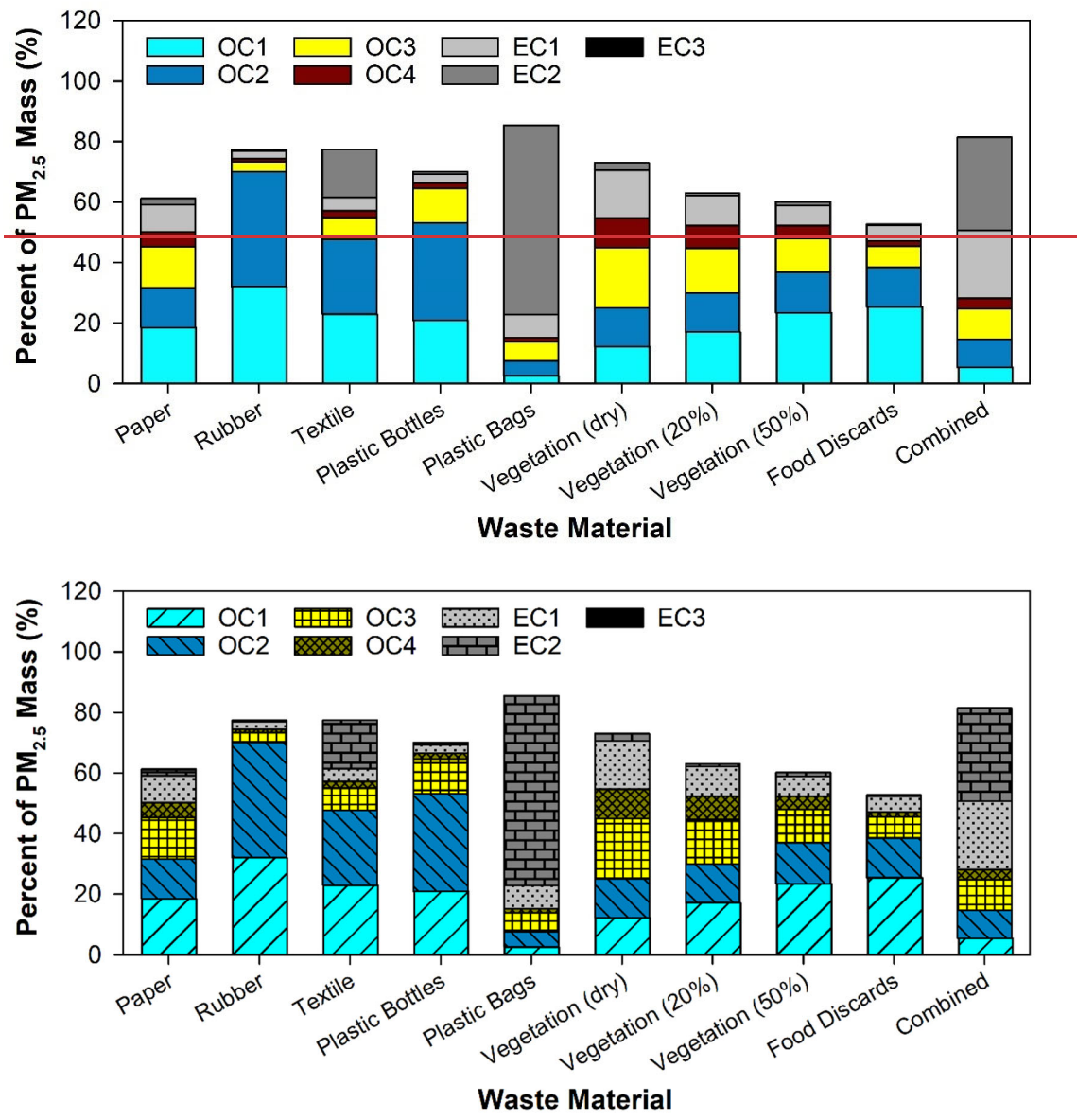
**Figure S3: Abundances of carbon fractions (% of PM$_{2.5}$ mass).**
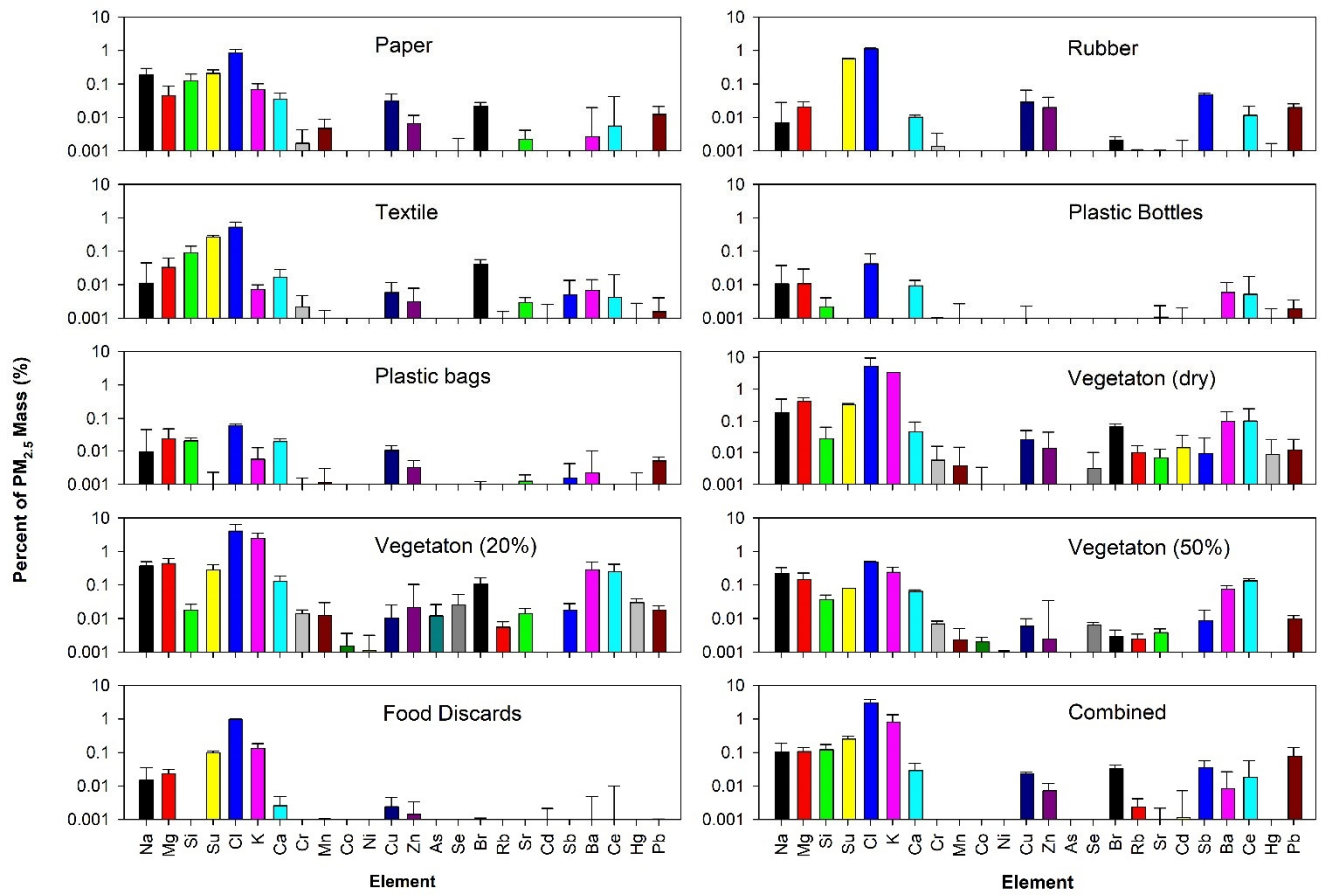
75    **Figure S4: Abundances of elements (% of PM$_{2.5}$ mass).**
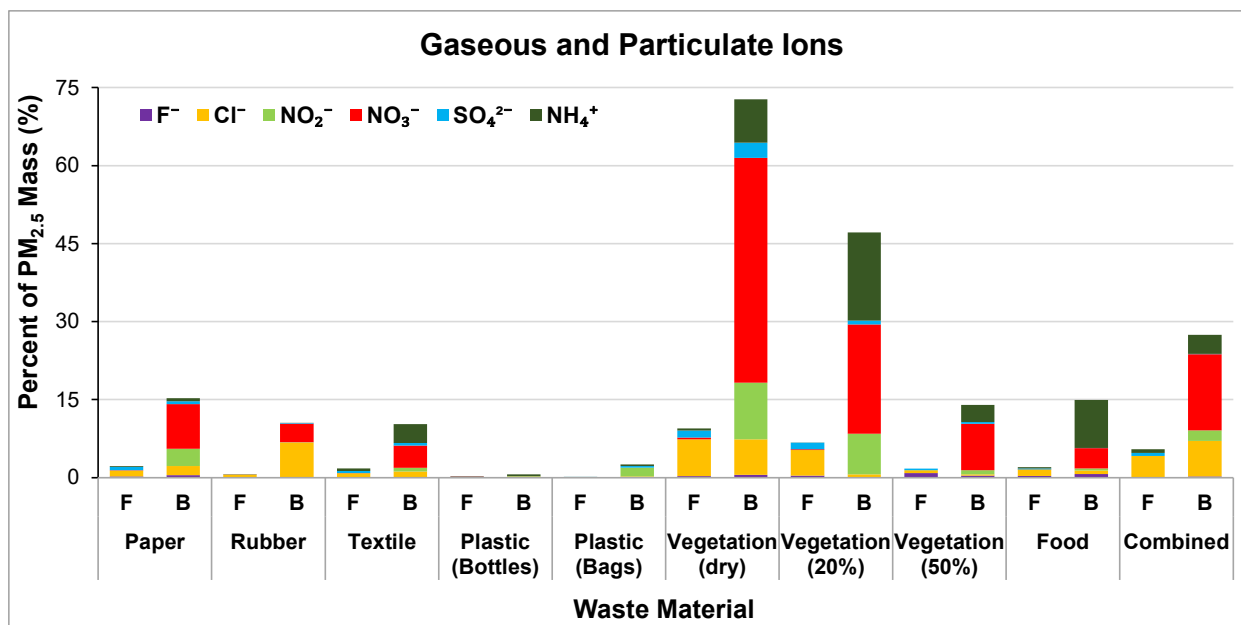
**Figure S5: Abundances of particulate ions captured on the front (F) quartz fiber filters and gaseous ions collected on the back (B) impregnated filters (see filter configuration in ~~Figure 1~~Figure 1). The sum of the particulate inorganic ions on the front filters was less than 10% of PM$_{2.5}$ mass for all waste materials. Among the three vegetations, particulate ions were most abundant in dry vegetation (9.9%), and their abundances decreased with increasing moisture content, likely due to lower combustion temperatures decreasing the generation of these ions. The gaseous ions were more abundant than particulate ions and the dry vegetation had higher gaseous ion than those with higher moisture content. The vegetation samples show high abundances of HCl, HNO$_2$, HNO$_3$, and NH$_3$. The rubber sample had a higher HCl abundance (6.7%) than for the other samples except for dry vegetation.**
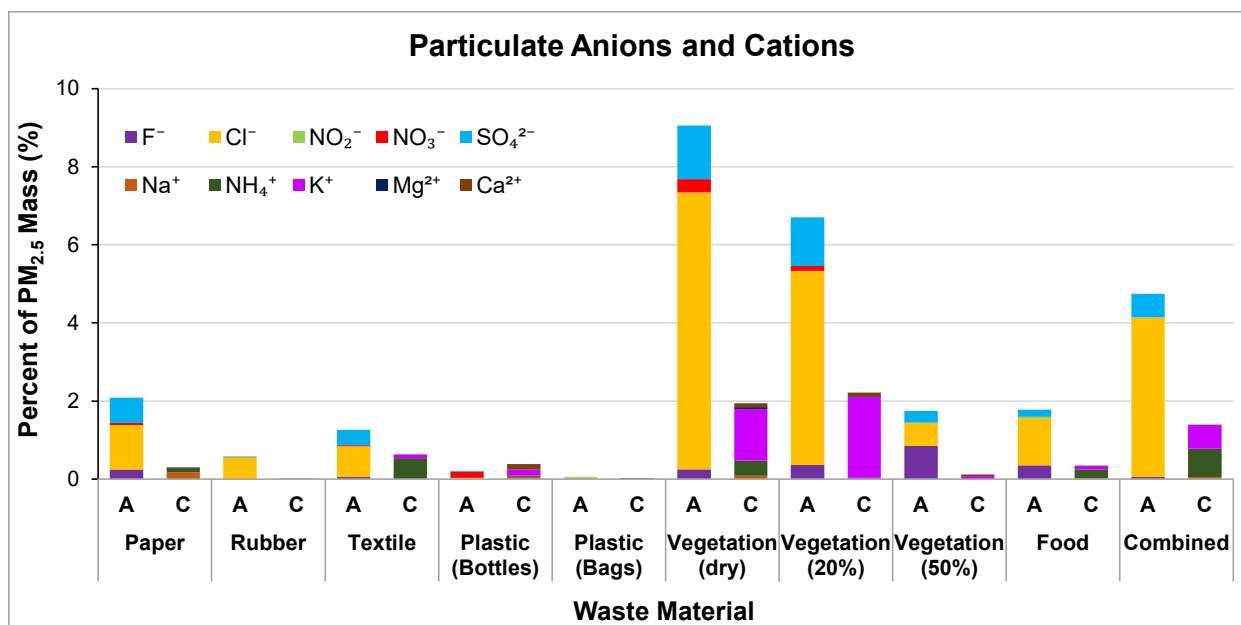
**Figure S6: Abundances of particulate anion (A) and cation (C) captured on the front quartz fiber filters (% of PM$_{2.5}$ mass).**

90
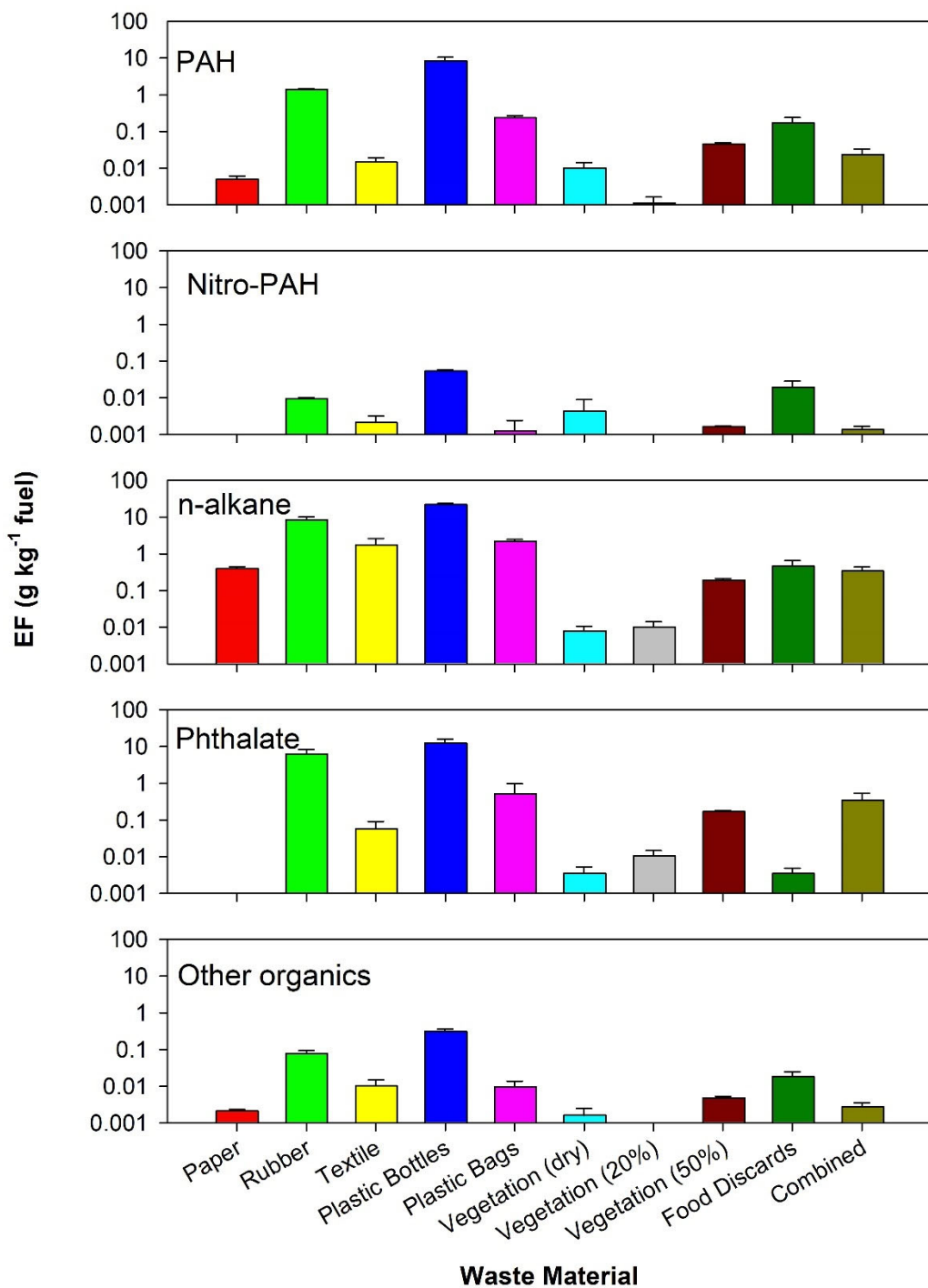
**Figure S7: Emission factors of organic species.**
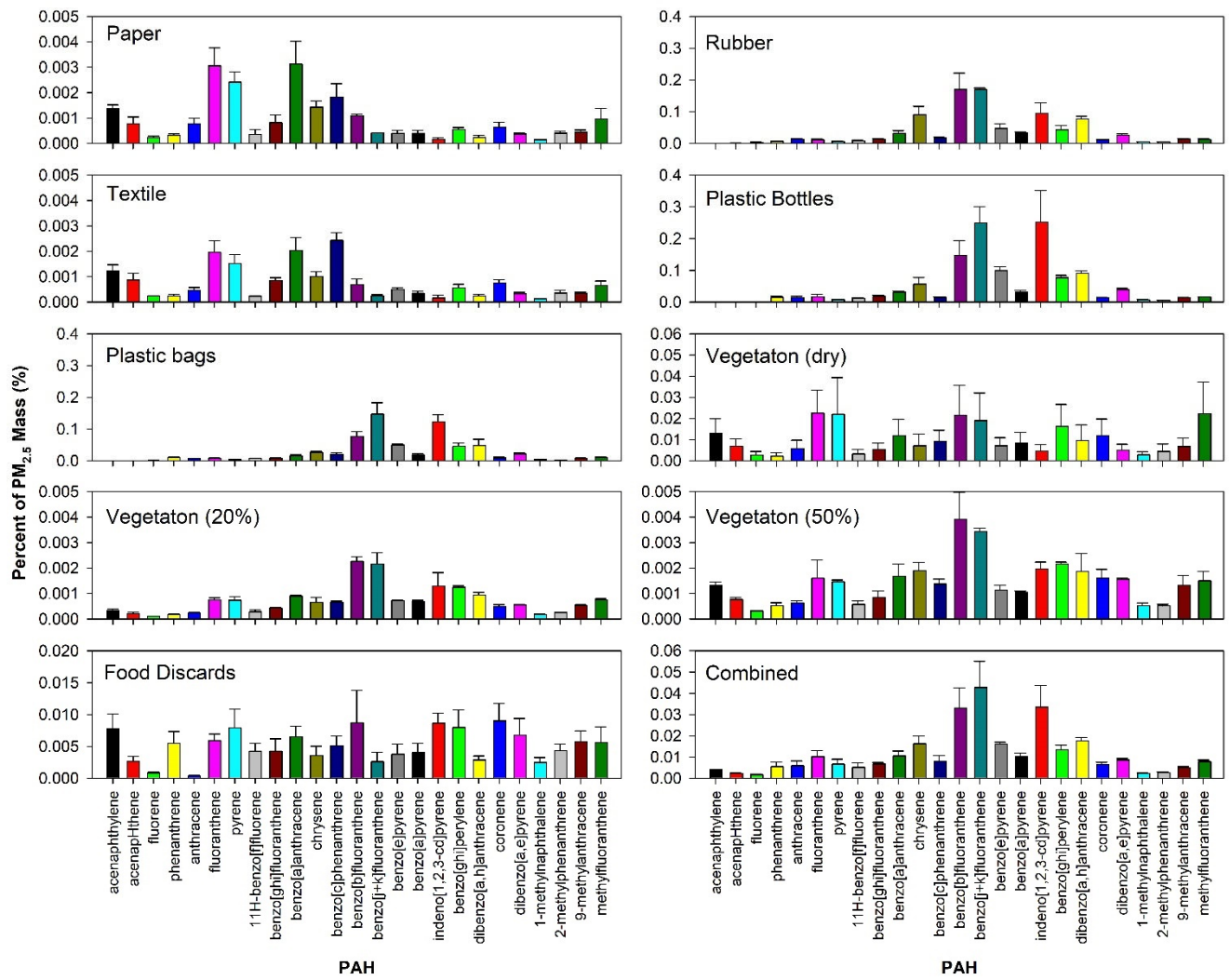
**Figure S8: Abundances of PAHs (% of PM$_{2.5}$ mass).**
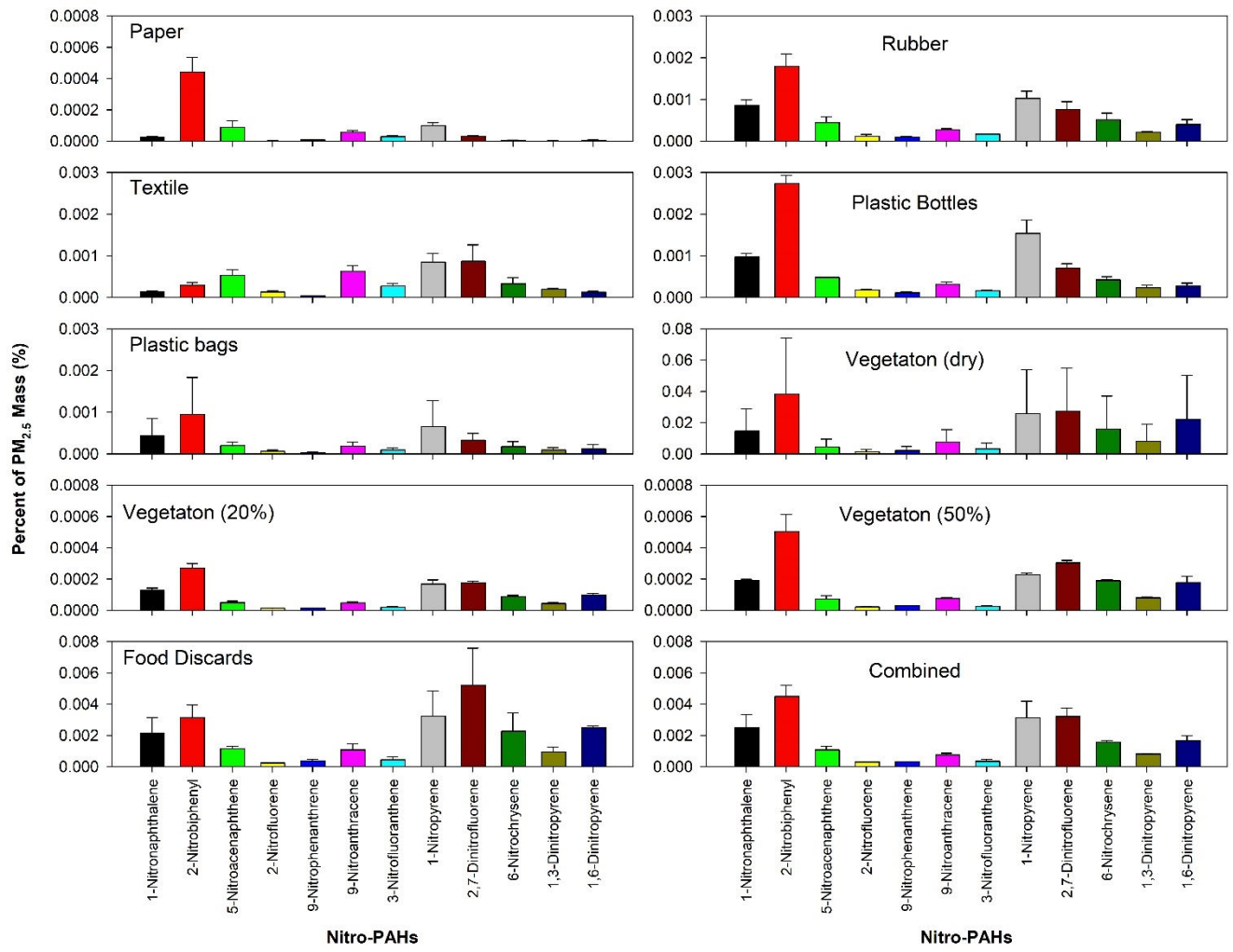
95      **Figure S9: Abundances of nitro-PAHs (% of PM$_{2.5}$ mass).**

S13
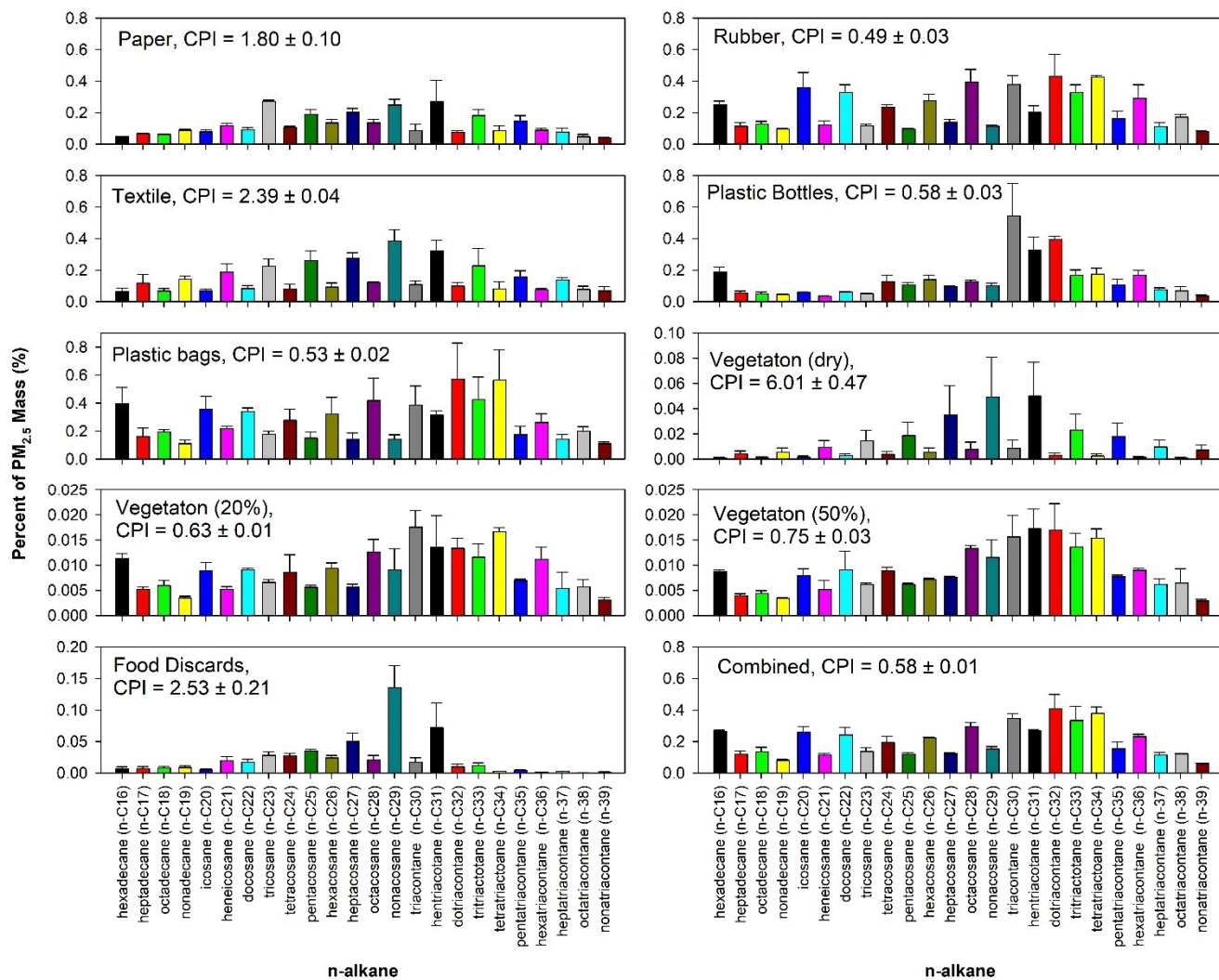
**Figure S10: Abundances of n-alkanes (% of PM₂.₅ mass).**
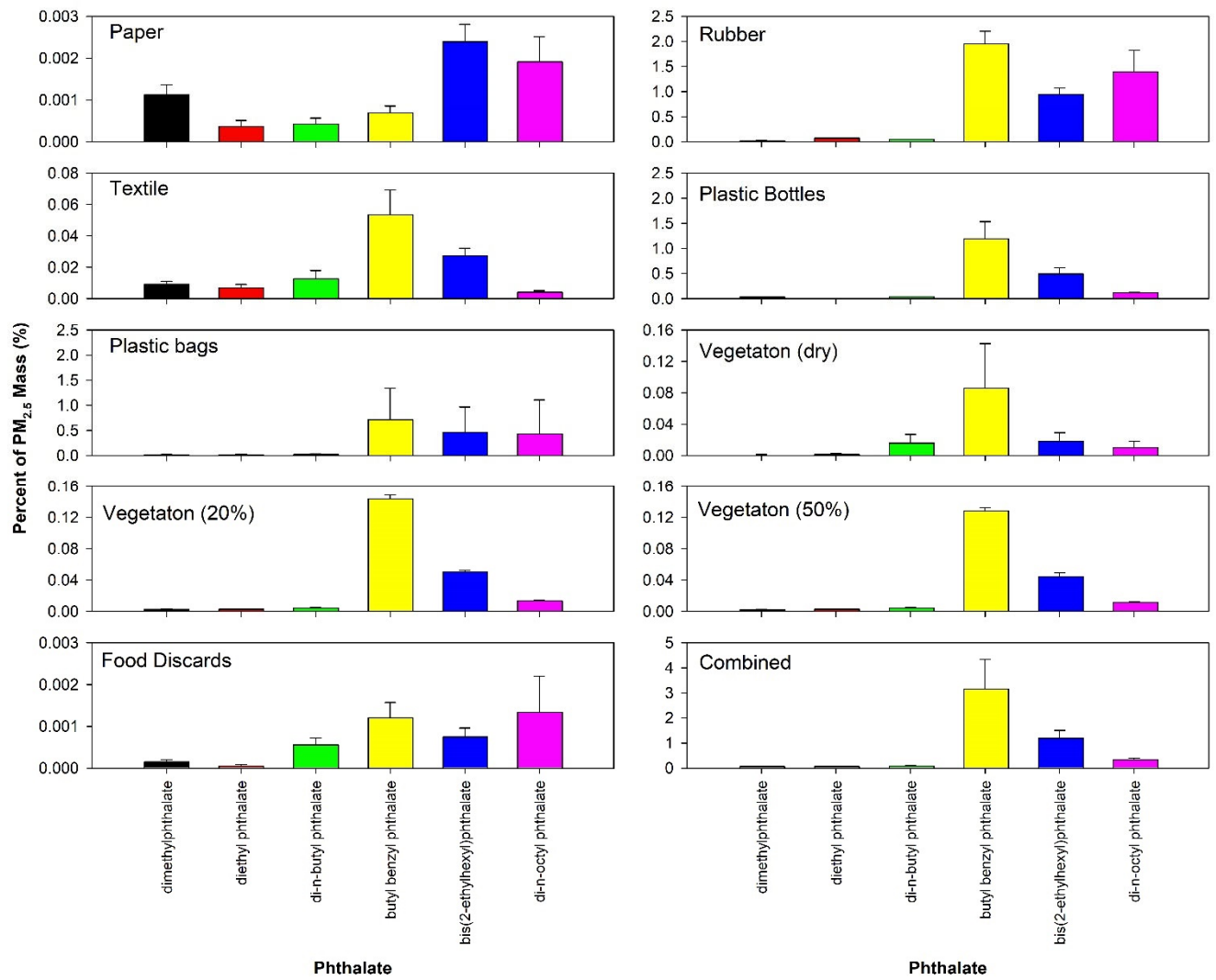
100    **Figure S11: Abundances of phthalates (% of PM$_{2.5}$ mass).**

S15